MASS TRANSFER IN SEMI-FLUIDIZED BEDS

by

Yung Chia Yang

B. S., National Taiwan University, China, 1955

A THESIS

submitted in partial fulfillment of the

requirements for the degree

MASTER OF SCIENCE

Department of Chemical Engineering

KANSAS STATE UNIVERSITY
OF AGRICULTURE AND APPLIED SCIENCE

1959

LD
2668
T4
1959
Y36
c.2
Documents

TABLE OF CONTENTS

INTRODUCTION 1

LITERATURE SURVEY 3

EXPERIMENTAL

Apparatus 15

Procedure 19

Materials 19

Analysis 20

Physical Constants 20

THEORY 33

RESULTS OF EXPERIMENTS 41

CORRELATION OF RESULTS 42

DISCUSSION 58

CONCLUSIONS AND SUMMARY 86

TABLE OF NOMENCLATURE 89

ACKNOWLEDGMENT 91

BIBLIOGRAPHY 92

APPENDIX 95

INTRODUCTION

'Semi-fluidization' is a new and unique fluid-solid contact operation in which the expansion of a fluidized solid particle bed is only partially allowed. The purpose of the present investigation was to study the mass transfer aspect of the process of 'Semi-fluidization' (9) (10).

The rate of mass transfer between solid particles and a flowing fluid is important in many chemical engineering operations, such as leaching, crystallization, and heterogeneously catalyzed reactions. In these applications, the solid particles may be disposed in either fixed or fluidized beds; both schemes have wide utility (8).

A state of fluidization results when the flow rate of fluid passing upward through a bed reaches a magnitude sufficient to buoy the solid particles and provide a sufficient space of free board inavailable for free upward expansion of the bed. The fluidized-bed operation has the following major advantages over the fixed bed operation: uniform exposure of particles to the fluid, ease of maintaining constant operation conditions due to the violent mixing action of solid and fluid, and more adequate removal and transport of particles from vessels than in fixed bed systems. However, the fluidization process is not immune to some serious defects of its own; such as loss of driving potential for the transport process within the bed which is largely due to the back-mixing of the solid particles and fluid; attrition and elutriation of the solid particles; requirement of considerable free board above the bed; and finally erosion of the walls of the containing vessel (8).

Recently it was proposed to partially eliminate those defects of the fluidized bed and to attain a type of solid-fluid contactor which compromises the feature of botb fixed and fluidized beds (9) (10). By partially restricting expansion of the fluidized bed, it was found that a definite fraction of the solid particles formed a fixed bed immediately below the top eieve plate, as shown in Plate I, and that the rest of the particles remained in a fluidized condition below the packed eection. The name of eemi-fluidization was taken from this pbenomenon (9) (10).

Such possibilitiee are suggested from many of the correlations of transport process (4) (24) within the solid-particle-fluid contactore, which are claimed to be equally applicable both to the fixed and to the fluidized bed. For instance, the mass transfer factor, jd, of Chu and his co-worker (4) suggests that, irrespective of the type of operation (fixed bed or fluidized bed), the rate of mass transfer can be altered if the porosity of the bed can be changed.

In the fixed bed, the porosity is a function of geometrical configuration of the particles and in the conventional fluidized bed, porosity ie a function of the characteristice of the solid particles and fluid, and the flow condition of the fluid and is not subject to arbitrary control. In other words, the porosity of a fluidized bed must be treated as a dependent variable rather than as an independent variable of the process. A typical set of available data on bed expaneion is plotted in Plate II in which the porosity of tbe beds ie plotted against the rate of fluid flow (8).

While the expansion in a conventional fluidized bed is unrestrained, in a 'Semi-fluidized bed' the bed expansion is restricted by a porous sieve plate introduced above the expanding bed thus forcing formation of a fixed bed above the fluidized bed. By adjusting the position of the top sieve plate, the overall bed porosity can be varied, and the desired heights of fixed and fluidized sections for optimum driving potential for mass, heat and momentum transfer may be obtained (9) (10). This means that the overall porosity of the semi-fluidized bed is a factor arbitrarily controllable within the limits of the rigidly fixed bed and fully fluidized bed and may be considered as an independent variable of the operation or process.

LITERATURE SURVEY

There is no published work available on any aspects of 'Semi-fluidization' except the one which reported the preliminary results of this investigation (9). However, the extensive theoretical and semi-empirical investigations have been done by Fan et al (10).

As mentioned in the previous section, a semi-fluidized bed contains both the fixed bed and fluidized beds simultaneously. The literature on mass transfer in fixed and fluidized beds prior 1954 was extensively reviewed by Chu (25). Therefore, only the major publications appearing before 1954 were reviewed, especially the ones which deal with the combined correlation of the mass transfer in both fixed and fluidized beds and the ones which contain information on the benzoic acid-water system.

EXPLANATION OF PLATE I

A picture of semi-fluidized bed

PLATE I

EXPLANATION OF PLATE II

Porosity of bed of benzoic acid particle fluidized with water (8)

Ordinate: ϵ , Porosity of bed, dimensionless

Abscissa: G, Liquid rate, lb/(hr.)(sq. ft.)

Legend:

○ , 8-10 mesh benzoic acid particle

● , 12-14 mesh benzoic acid particle

△ , 20-24 mesh benzoic acid particle

▲ , 24-28 mesh benzoic acid particle

PLATE II

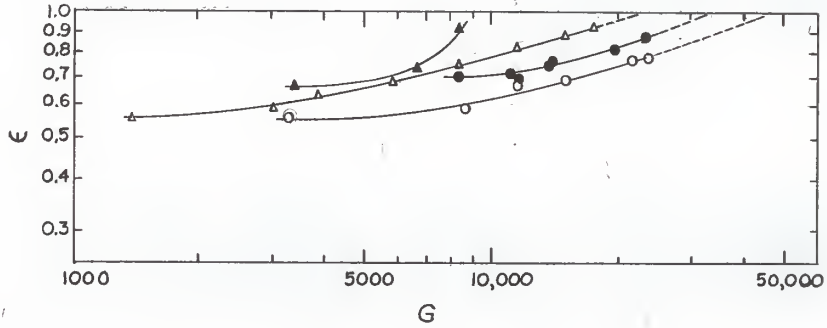

Gamson, Thodos and Hougen (15) made psychrometric measurements for studying the rate of evaporation of water from spherical and cylindrical porous pellets into air streams. In their work, porous pellets were soaked in water usually for several hours, the excess water was drained off, the pellets were rolled in cheesecloth to remove the excess adhering water on the surface and without removal of capillary moisture. It was, therefore, expected that the interfacial surface area between the gas stream and the liquid was different from the geometric surface area of the solids on which the mass transfer coefficients calculated by Gamson et al., (15) were based. Bed thicknesses not exceeding 2 1/2 in. were used with particle sizes as large as 3/4 in. In such shallow beds the entrance and exit effects and axial mixing effects might play important roles. Moreover, the height and the fractional void volume for a bed made up of a few layers of solids are quantities of questionable significance. The data were presented by plotting the jd factor against the Reynolds number, GD_p/μ . The following equations were used to correlate their data:

$$J_d = 0.989 \left(\frac{D_pG}{\mu}\right)^{-0.41} \qquad \text{for } \frac{D_pG}{\mu} > 350 \qquad (1)$$

$$J_d = 16.8 \left(\frac{D_pG}{\mu}\right)^{-1} \qquad \text{for } \frac{D_pG}{\mu} < 40 \qquad (2)$$

Additional data to those of Gamson, Thodes and Hougen (15) were obtained by Wilke and Hougen (34) for the purpose of investigating further the region of lower gas flow rate. Equation (2) was replaced with the following equation:

$$J_d = 18.2\left(\frac{D_pG}{\mu}\right)^{-0.51} \qquad \text{for } \frac{D_pG}{\mu} < 100 \tag{3}$$

Hurt (18) studied the following systems; (a) the adsorption of water vapor from moist air by particles of silica gel and by particles coated with phosphorous pentoxide, (b) adiabatic humidification of air over silica gel pellets wetted with water, (c) evaporation of naphthalene flakes into air and hydrogen streams. The results for (a) were considered doubtful. Data were given for case (b) and (c) together with the results obtained from calculationf of Ht. The fractional void volumes were not measured. It was reported as follows:'' . . for different size particles of similar shape no satisfactory correlation of the data into a single curve could be obtained. Data are, accordingly, presented as separate curves for each size and shape investigated.'' The author apparently did not recognize that the plot of Ht/Dp against D_pG/μ would bring the data for different sizes into a single line.

Rates at which naphthalene was vaporized into air, hydrogen, and carbon dioxide streams from fixed and fluidized beds were measured by Resnick and White (27). In their fluidized bed correlation of jd factor against Reynolds number, two modes of fluidization were noted; an initial smooth bubbling type where the jd factor increased with increasing N'_{Re}. Mesh size appeared as a parameter on a plot of jd vs. N'_{Re} and Resnick and White correlated their data in the slugging region by replotting $Jd/N_{Sc}^{0.57}$ against N'_{Re}/ϕ. Where ϕ is the dimensionless group:

$$\frac{D_p^3 P_g G(P_s - P_g)}{U^2}$$

Studies by Taecker and Hougen (31) were identical with those of Gamson, et al. (15), and Wilke and Hougen (34), except that Raschig rings and Berl saddles were used instead of spheres and cylinders. The effective particle diameter, D_p', for the spherical shape packings used, was calculated by $D_p' = \sqrt{A_p/\pi}$, where A_p is the dry surface area for one packing unit. Even with this modification, the j_d factors for Raschig rings and partition rings were 19% lower than those for solid spheres and cylinders. Berl saddles gave valves about 30% higher than for the rings. In order to correlate their data the following equations were developed:

$$J_d = 1.251\left(\frac{GD_p'}{\mu}\right)^{-0.44} \qquad \text{for } \frac{GD_p'}{\mu} < 620 \qquad (4)$$

$$J_d = 2.24\left(\frac{GD_p'}{\mu}\right)^{-0.51} \qquad \text{for } \frac{GD_p'}{\mu} > 620 \qquad (5)$$

Hobson and Thodos (17) passed water through a bed of celite spheres presoaked in a saturated solution of either water in isobutyl alcohol or of water in methyl ethyl ketone. The variation of the effluent concentration with time was measured so that the transfer rates would be calculated at "zero time" when the particles were believed to be completely wetted by saturated solution. The questions that concerned Gaffney and Drew (13) were: (1) how accurate was the extrapolation to a somewhat uncertain "zero time" for a curve of rapidly changing slope? (2) did the pellets have excess solution on their surface initially? (3) if not, how were they removed without depleting the surface? The following generalized equation, correlating also the data of Gamson, Thodos and Hougen (15) and Wilke and Hougen (34) was recommended by Ergun (7):

$$\log J_d = 0.7683 - 0.9175 \log(N'_{Re}) + 0.0817 \left[\log N'_{Re}\right] \qquad (6)$$

McCune and Wilhelm (23) studied the mass transfer ratee from 2-naphthel pellets into water etreams. The work of these authors conetituted an excellent investigation free from most of the uncertaintiee of the earlier studies. Use of uniform size pellets assured accurate estimation of the geometric surface area of the solids which constituted both the surface exposed to flow and the interfacial surface for mass transfer. Ample bed heights were used. The fraction void volumes of the fixed beds could have been easily calculated from the bulk densities, ρ_b, and the particle density of the pellets, ρ_s, by the use of the relationship $\epsilon = 1 - \frac{\rho_b}{\rho_s}$. This, however, apparently was overlooked by the authors, who determined the fractional void volume for each type of packing in a eeparate apparatus, although the pellets may not have been packed to the same bulk densities in the separate container. Data were presented as a plot of the j_d factor against Reynolds number, and data were represented by two straight lines:

$$J_d = 1.625\left(\frac{D_pG}{\mu}\right)^{-0.507} \qquad \text{for } \frac{D_pG}{\mu} < 120 \qquad (7)$$

$$J_d = 0.687\left(\frac{D_pG}{\mu}\right)^{-0.327} \qquad \text{for } \frac{D_pG}{\mu} > 120 \qquad (8)$$

Evans and Gerald (8) measured mass-transfer coefficients for fixed and fluidized beds of benzoic acid granules dissolving in water. Four different sizes of benzoic acid granules were used. By empirically modifying an application of the Reynolds analogy, the fluidized-bed data were all correlated by a single line, with mass velocity as the only flow

variable. To express the data the following equation was developed:

$$J_d \frac{(1-\epsilon)(Dp)2.6}{f'} = 2.3 \times 10^{-10} (N'_{Re})^{1.33} \quad (9)$$

Chu, et al. (14) presented mass-transfer data for transfer between regular shaped solids and a turbulent gas stream for both fixed and fluidized granular beds, and a simple generalized correlation was achieved. In contradiction to two previous investigations on gas-solid fluidized beds, the data were found to be in agreement with practically all the fixed bed data of widely varying systems, as well as with data for fluidized liquid-solid and gas-solid beds. The equations for mass transfer could be written as:

$$J_d = 5.7 \left[D_pG/\mu \ (1-\epsilon)\right]^{-0.78}; \quad 30 > \left(D_pG/\mu \ (1-\epsilon)\right) > 1 \quad (10)$$

$$J_d = 1.77\left(D_pG/\mu \ (1-\epsilon)\right)^{-0.44} 10{,}000 > \left(D_pG/\mu \ (1-\epsilon)\right) > 30 \quad (11)$$

The Chilton and Colburn (3) analogy of mass transfer and pressure drop for flow in conduits was modified for flow in granular beds. The resulting relation holds remarkably well over a wide range of Reynolds and Schmidt numbers, making possible the prediction of mass transfer data in granular beds from the more easily obtainable pressure drop data. The equation relating mass and momentum transfer is simply stated as $j_d = f/10$.

Ishine, Otake and Okada (20) studies mass transfer between solid benzoic acid particles in fixed beds with upward and downward flowing streams of waters. The range of experimental and correlative variables were as follows: particle shape and size, 3.5, 4.5 and 5.5 cm. cylinders with equal diameter and height; Reynolds number, 1 to 140; Schmidt numbers,

1180 to 1610; fixed bed depth, 1.3 to 13 cm. The correlated results using j_d factor and Reynolds number were:

$$J_d = 2.1 \, (N'_{Re})^{-0.80} \qquad \frac{D_p G}{\mu} < 5 \tag{12}$$

$$J_d = 1.44 \, (N'_{Re})^{-0.507} \qquad 5 < \frac{D_p G}{\mu} < 140 \tag{13}$$

Shirai, (30) used the data obtained by several investigators (13) (17) (23) and obtained a single line correlation of the fixed beds, fluidized beds and single particle data. Shirai (30) plotted $N_{Sh}\epsilon$ vs $N'_{Re}N_{Sc}^{1/3}$ for mass transfer and similarly $N_{Nu}\epsilon$ vs $N'_{Re}N_{Pr}^{1/3}$ for heat transfer. These can be expressed by equations:

For mass transfer $$N_{Sh}\epsilon = 2.0 + 0.75 \, N'^{1/2}_{Re} N_{Sc}^{1/3} \tag{14}$$

For heat transfer $$N_{Nu}\epsilon = 2.0 + 0.75 \, N'^{1/2}_{Re} N_{Pr}^{1/3} \tag{15}$$

Recently, Wakao and others (32) further modified Shirai's mass transfer equation to the expression:

$$N_{Sh} = 2.0 \quad 0.52 \; N'^{0.54}_{Re} N_{Sc}^{0.35} \tag{16}$$

Galleway et al., (14) studied the effect of packing configuration on mass and heat transfer in beds of stacked spheres. Experimental measurements were reported on the simultaneous rates of mass and heat transfer for the surface evaporation of water into air from two orthorhombic, one rhombohedral, and two simple cubic assemblages of uniform celite spheres, in the Reynolds number range 300-1200. The measurements were confined to the pre-determined constant rate drying period of the spheres. No appreciable differences in mass or heat transfer factors were found for the various assemblages, except for the cubics, which exhibited slightly

lower transfer factors than the other assemblages at the higher Reynolds number. The negative slope of the log. j vs. log. Re curves was designated the "index of turbulence inhibition". This index was correlated with the projected fractional free area of the packings, as well ae with the wall effect. Various methods proposed by investigators of randomly packed beds for modifying the mass transfer factor and/or the Reynolds number failed to improve the overall correlation of the results. The inapplicability of a simple analogy between momentum and mass transfer, as proposed by Ergun (7) was demonstrated.

Wakao and others (32) studied mass transfer rates from spherical and cylindrical 2-naphthel particlee to water in packed beds. Data at low water velocities show that Sherwood number tends to approach 2.0 with decrease of N'_{Re}. His data and the previouely published data of other investigators (8) (23) for spherical and cylindrical particles were generalized and correlated by:

$$N_{Sh} = 2.0 + 1.45\, N_{Sc}^{1/3}\, N_{Re}^{1/2} \qquad N'_{Re} \quad 100 \tag{17}$$

$$N_{Sh} = 2.0 + 0.90\, N_{Sc}^{1/3}\, N_{Re}^{0.60} \qquad N'_{Re} \quad 100 \tag{18}$$

The data for flakes (23) and broken solids (8) for the experimental range of $N'_{Re} > 1$, agree with the results obtained from above the equations.

Wakao et al., (33) obtained the axial turbulent diffusion coefficients by measuring axial concentration gradients in water-fluidized beds of cylindrical 2-naphthel particles. When the concentration in the bed is very small as compared with the saturation concentration, the dissolution rate approximates a zero-order reaction expressed as:

$$U_o \frac{dc}{dl} = E_Z \frac{d^2c}{dl^2} + kpaC_s \qquad (19)$$

By using the boundary condition at the inlet and outlet of the bed, that is

$$\text{inlet } l = 0 \quad U_oC = E_Z (dc/dl) \qquad (20)$$

$$\text{outlet } l = L \quad dc/dl = 0 \qquad (21)$$

Equation (22) can be derived from equation (19)

$$\frac{C_n}{C_L} = n + \frac{E_Z}{U_oL}\left[1 - \exp\left\{\frac{U_oL}{E_Z}(1 - n)\right\}\right] \qquad (22)$$

in which l is axial distance, L is bed height and $n = l/L$

EXPERIMENTAL

Apparatus

The experimental apparatus consisted of a main test column in which granular benzoic acid particles were dissolved by a measured stream of upward flowing water, and a container for retention of samples of each run for analysis. The diagram of apparatus is shown in Plate III.

Ordinary water was supplied from a 50-gallon constant-head tank (A). Water from the tank was forced through the system by a centrifugal pump (B). The water was initially directed through a globe valve and a Brooks type 1110 flowmeter (C) as a means of controlling and measuring the rate of flow. The test column consisted of two parts, a calming section (D) and a test section (F). The calming section was a pyrex tube, 4 inches inside diameter, 12 inches high, and packed with Raschig rings and Berl saddles to maintain even distribution of flow. The test section was a

vertical pyrex tube, 2 inches inside diameter and 24 inches high. Two braes plates clamping a filter cloth (E) were placed between the calming and the test eections in order to establish an even distribution of the upward flow. A rigid close-fitting sieve plate (G) was attached to a long rod which could be moved up or down to a fixed position. This was installed in the test column in order to adjust bed depth and prevent the complete expansion of the eolid bed. The emall holes in this sieve plate were punched evenly in order to obtain a uniform packed section above the fluidized section. Otherwise, an inclined surface would appear between the two phasee. The outlet line consisted of half-inch tubing, which carried the product to the retention tank.

In order to carry out two series of experiments in the present investigation, the apparatue was modified.

In the first series, only the inlet and outlet concentrations were measured and in the second eeries, the axial concentration gradient of the fluid was measured. The apparatus used in the later series was the same as those used for the former series, except the teet eection. This new teet section was made from a 2-inch inside diameter standard iron pipe with cocks attached for sampling, at 2 inch spacings. A sheet of filter cloth was attached by Duce cement to the inside wall over the outlet of each cock. This was intended to prevent the solid benzoic acid particles from plugging the sampling cocks. This is illustrated diagramatically in Plate III.

EXPLANATION OF PLATE III

Schematic diagram of experimental apparatus

Legend:

A. Water tank

B. Pump

C. Flowmeter

D. Calming section

E. Filter cloth

F. Test section

G. Top sieve plate

H. Sampling outlet

I. Retention tank

PLATE III

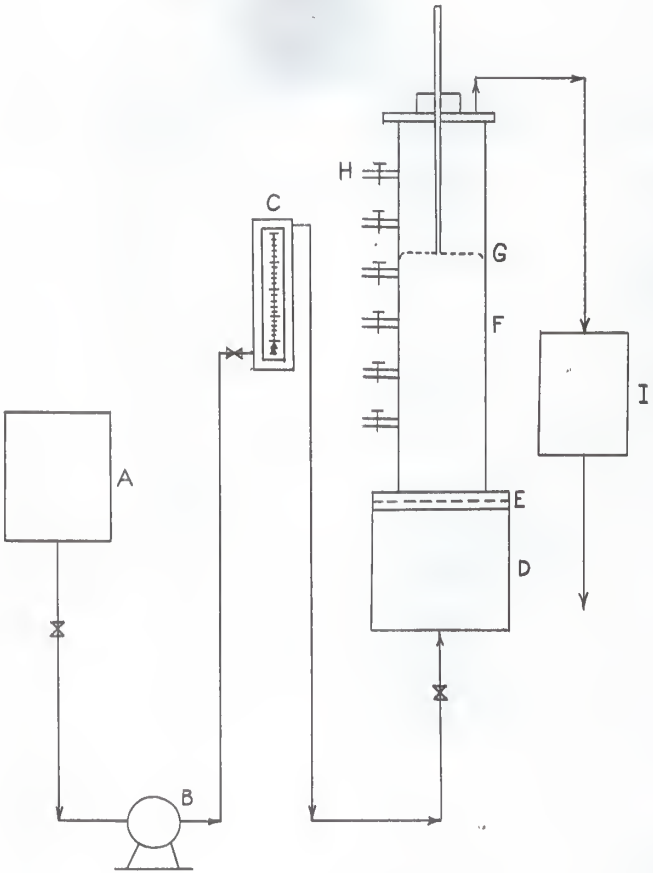

Procedure

At the start of the operation, water was gradually run into the bottom of the calming eection. The flow rate was regulated in such a way that air bubbles were eliminated in the inert packing material. Some difficulty wae often encountered in removing air bubbles and emall crystals from the teet section but careful manipulation of the flow rate overcame theee problems.

The solubility of the benzoic acid in water is low and in order to minimize the change of geometric shape of the particles during the experimental runs, the individual runs were not permitted to exceed an 80 seconds duration. A decrease of less than three per cent of the initial weight of the eolid particles for a single run was experienced.

In a single run, a top-to-bottom sampling sequence was followed for determination of the concentration gradients. The advantage of a top-to-bottom sampling sequence was due mainly to the fact that there would be no influence in concentration gradient in the lower eection of the fluid while the fluid from the upper region was being drawn off. If a reverse order were adopted, concentration gradients would vary appreciably and cause experimental errors due to the influence of the side stream sampling.

All the experimente were carried out at room temperature and the fluid temperature was measured at the inlet and outlet of the column.

Materials

Granular particles of benzoic acid were prepared in three Tyler screen ranges; 8-10 mesh, 12-14 mesh and 2-24 mesh. U.S.P. benzoic acid

was melted in large cast, broken up in small lumps, and finally ground in a Braun Pulverizer type crusher. The particlee were ecreened in a Rotap ehaker. Undesired screen fractions were remelted and reground. Adhering dust wae removed and surface wetability improved by contacting the bulk preparation of each size with a large volume of dietilled water. The particles were eubeequently air-dried to constant weight (1).

Analyeis

The determination of the concentration of the water sampler wae made by direct titration ueing 0.04 N. sodium hydroxide with phenolphthalein indicator. No difficulty was encountered in securing a reproducible end-points. The acid concentration varied from 0.0004 gm. acid per gm. of water to 0.0030 gms. acid per gm. of water.

Physical Constants

The physical constants used in the present investigation are briefly summarized below:

1. Solubility, C_s:

The saturation concentration of benzoic acid in water for use in evaluating driving force was obtained by reviewing all the available data in the literature (29) (19). Although there was a fair amount of disagreement, a sufficient number of substantiated values were found for the required temperature range to insure sufficient accuracy for this work. Solution saturated with the benzoic acid used in the present investigation was found by titration to be in agreement with the literature value (29). A plot of solubility related with temperature is shown in Plate IV. Also

EXPLANATION OF PLATE IV

Solubility of benzoic acid in water

Ordinate: C_s, Solubility, gm./liter

Abscissa: T, temperature, ^{o}C

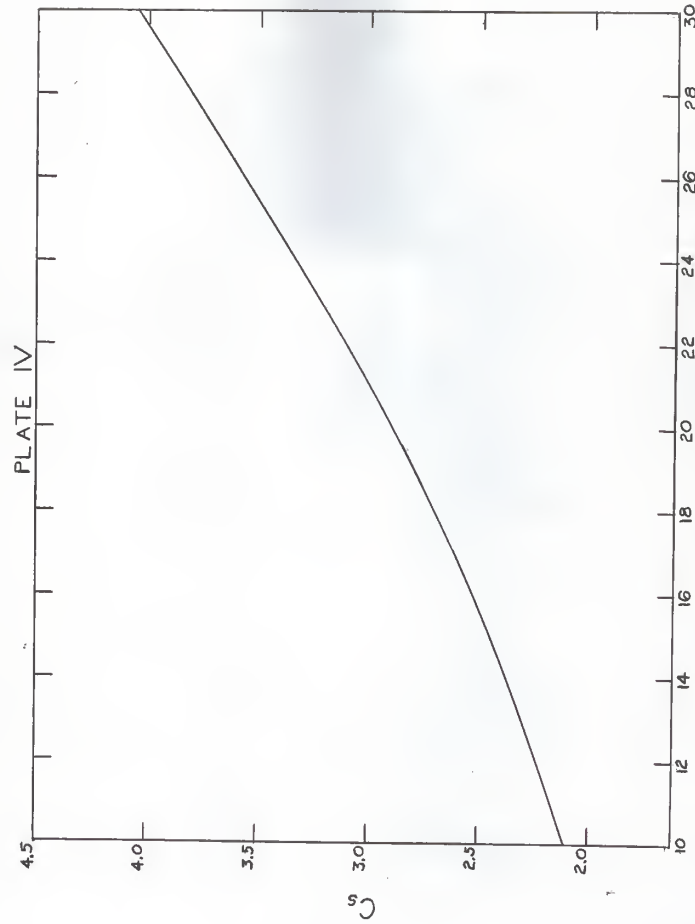
PLATE IV
C_s
4.5
4.0
3.5
3.0
2.5
2.0
10
12
14
16
18
20
22
24
26
28
30
T

solubility can be represented by an equation reported by Ishine (20) as function of temperature:

$$C_s = 0.17 + 0.00197t + 0.000202t^2 \quad (t: 0^\circ - 30^\circ C) \qquad (23)$$

2. Diffusivity, D_v: and Schmidt Number μ/PD_v

The Diffusivity and Schmidt number were taken directly from the data of Chang (2), quoted by Linton and Sherwood (22). Values of the Schmidt number at four temperatures were reported. A smooth reference curve, Plate V, VI, was plotted from these values.

3. Viscosity, μ:

Since the concentrations of benzoic acid solution obtained in this work were very low, water viscosity was employed to calculate Reynolds numbers (26).

4. Density of particle, ρ_s:

The density of particles was measured by weighing a sample of particles and adding it to a graduated volumetric cylinder. A known volume of saturated benzoic acid solution was added. The total volume of the particles plus added liquid was read and the volume of particles was determined by the difference to an accuracy sufficient for this work. The value determined was 1.293 gm./ml., somewhat above the literature value of 1.266 (19).

$$\rho_s = \frac{\text{Weight of benzoic acid}}{\text{Total volume} - \text{Volume of saturated benzoic acid solution}} \qquad (24)$$

EXPLANATION OF PLATE V

Diffusivity of benzoic acid in water

Ordinate: $D_v \times 10^5$, Diffusivity, $cm^2/sec.$

Abscissa: T, Temperature, ^oC

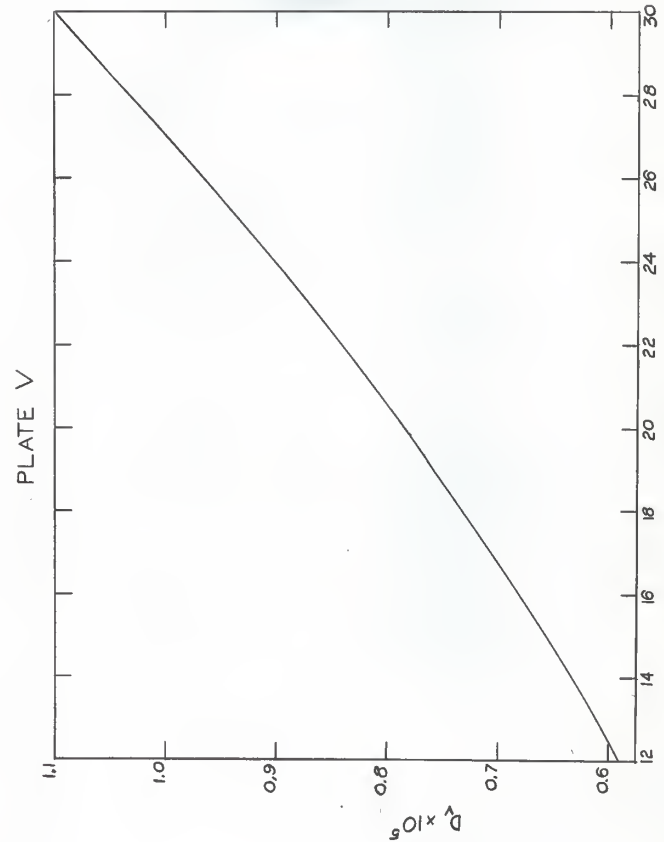
PLATE V
$D_v \times 10^5$
1.1
1.0
0.9
0.8
0.7
0.6
12
14
16
18
20
22
24
26
28
30
T

EXPLANATION OF PLATE VI

Schmidt number of benzoic acid in water

Ordinate: N_{Sc}, Schmidt number, dimensionless

Abscissa: T, Temperature, ^{o}C

PLATE VI

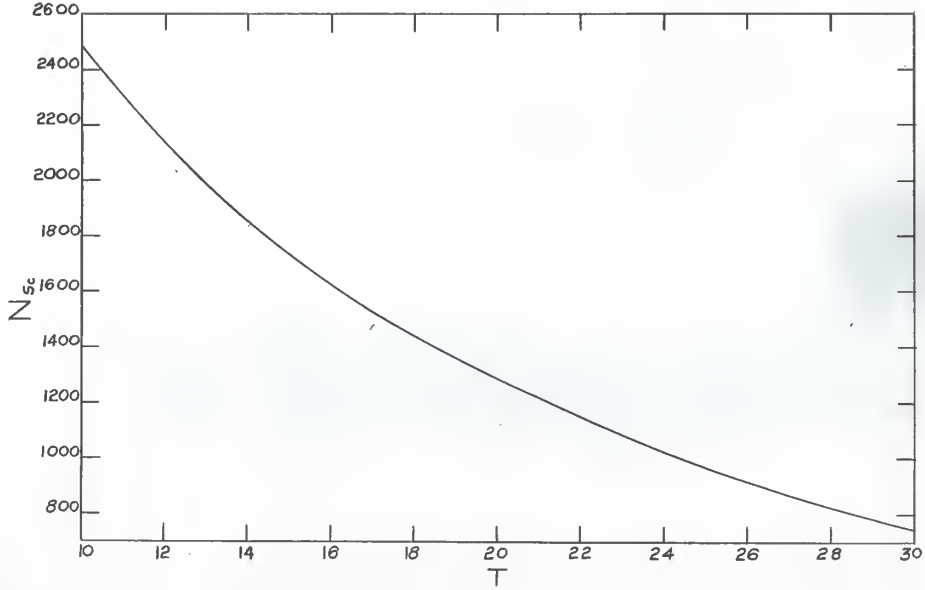
2600
2400
2200
2000
1800
1600
1400
1200
1000
800
N_{sc}
10
12
14
16
18
20
22
24
26
28
30
T

5. Bulk density of particles, ρ_b:

The bulk density of particles was measured by weighing a sample of particles and adding it to a graduate volumetric cylinder. The volume of particles was directly readed. Plate VII showed the relationships between bulk density of particles and particle diameter for benzoic acid particles.

$$\rho_b = \frac{\text{Weight of benzoic acid}}{\text{Volume occupied by benzoic acid particles}} \tag{25}$$

6. Particle size, D_p:

The particle sizes reported here were the diameter of an equivalent sphere, having the same volume as the particles.

$$D_p = \left(\frac{6}{\pi} \quad \frac{\text{Average weight of particle}}{\rho_s} \right)^{1/3} \tag{26}$$

7. Shape factor, ϕ:

The shape factor of the particles, defined as the ratio of the surface area of the equivolume sphere to the surface area of the actual particle, varied from 0.50 to 0.65. A plot of shape factor against particle diameter was shown in Plate VIII.

$$\phi = \frac{\pi D_p^2}{\text{Surface area of particle}} \tag{27}$$

8. Specific surface, S_o:

The specific surface is defined as the ratio of surface area of the equivolume sphere to the volume of the particle, and was determined by measuring the pressure drop for a measured flow rate of saturated benzoic

EXPLANATION OF PLATE VII

Bulk density of benzoic acid related to the particle diameter

Ordinate: ρ_b, Bulk density, lb./cu.ft.

Abscissa: D_p, Particle diameter, ft.

PLATE VII

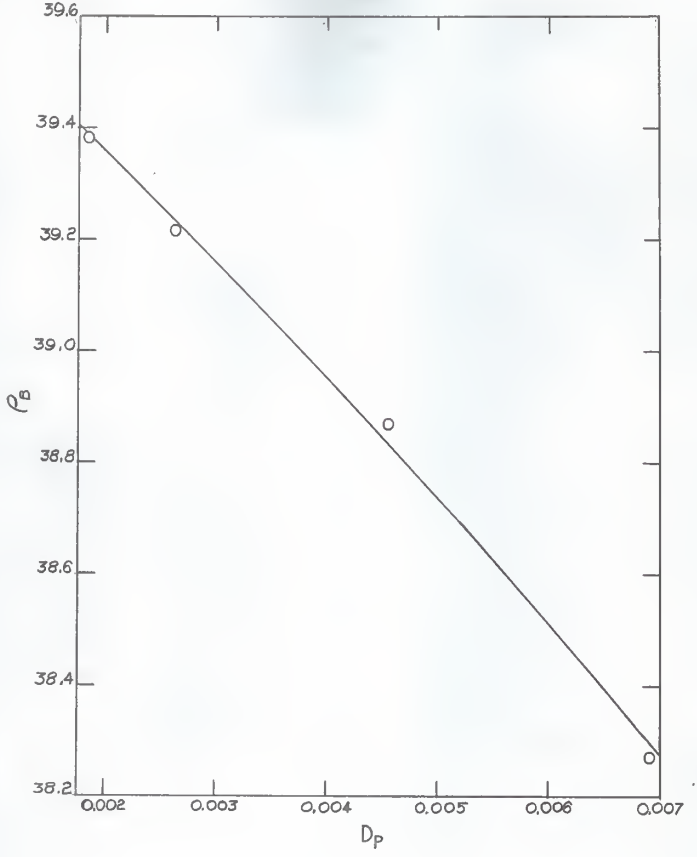
39.6
39.4
39.2
39.0
38.8
38.6
38.4
38.2
ρ_B
0.002
0.003
0.004
0.005
0.006
0.007
D_P

EXPLANATION OF PLATE VIII

Shape factor of benzoic acid related to the particle diameter

Ordinate: ϕ, Shape factor, dimensionless

Abscissa: Dp, Particle diameter, ft.

PLATE VIII

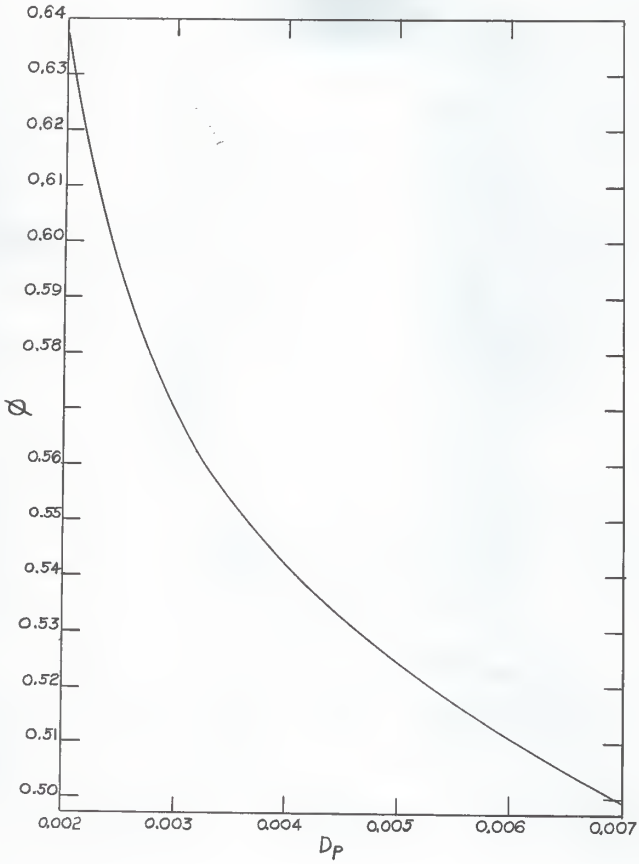
0.64
0.63
0.62
0.61
0.60
0.59
0.58
Q
0.56
0.55
0.54
0.53
0.52
0.51
0.50
0.002
0.003
0.004
0.005
0.006
0.007
D_P

acid solution through a bed of particles. The equipment used for this purpose was similar to that of Carman (1) and his equation relating surface area to pressure drop was used.

$$S_o = \frac{6}{D_p \phi} \tag{28}$$

9. Porosity of solid particle bed, ϵ :

The porosity of solid particle bed is defined as the ratio of the volume of voids in the bed to the total volume of the bed. It may be evaluated as one minus the ratio of bulk density to its solid density as:

$$\epsilon_o = 1 - \frac{\rho_b}{\rho_s} \tag{29}$$

When the bed expands from h_o to h_f, the porosity becomes:

$$\epsilon = 1 - \frac{1 - \epsilon_o}{R} \tag{30}$$

where R is the ratio of the original bed height to the expanded bed height.

In the present work, the bulk density of the dumped particle bed was used to calculate the porosity of the packed bed. This porosity may be defined as the dumped porosity or dumped void, and can be considered as the porosity of a most loosely and randomly packed bed. It is shown in Plate IX. The properties of benzoic acid particles used in this investigation are listed in Table I.

THEORY

To derive the rate equation for the mass transfer between the solid particles and fluid, the following assumptions were made:

EXPLANATION OF PLATE IX

Dumped void related to the particle diameter

Ordinate: ϵ_o, Dumped void of particle, dimensionless

Abscissa: Dp, particle diameter, ft.

PLATE IX

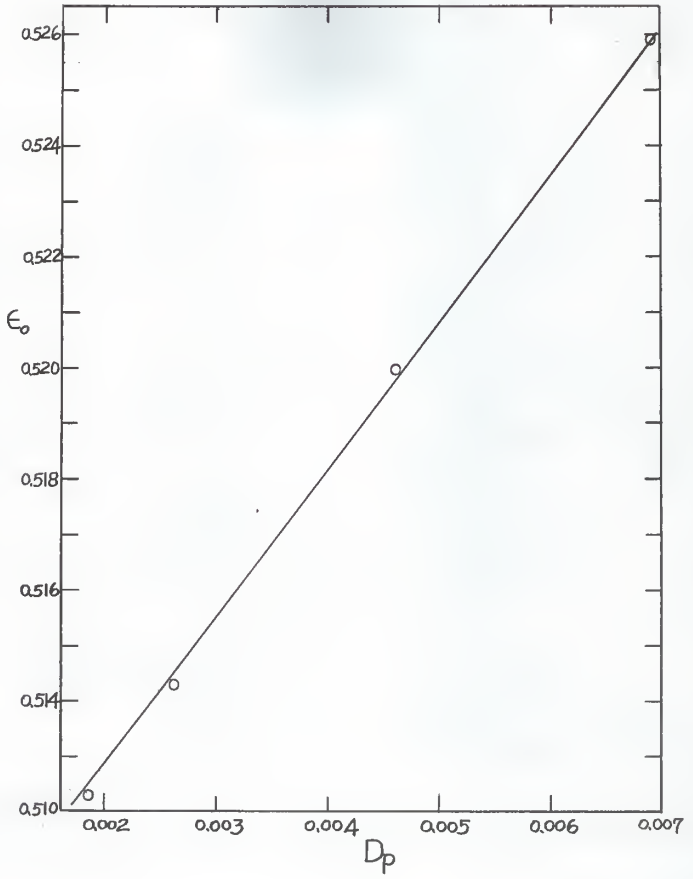
0.526
0.524
0.522
ϵ_o
0.520
0.518
0.516
0.514
0.510
0.002
0.003
0.004
0.005
0.006
0.007
D_p

Table 1. Properties of benzoic acid particle

Tyler Screen Mesh	No. per gram	Bulk density lb/ft^3	S_o, ft^{-1}	Dp, ft.	Shape factor	ϵ_o
8-12	156.5	38.2757	1720	0.00693	0.500	0.5259
12-14	545	38.7128	2480	0.00456	0.531	0.5205
20-24	2870	39.2123	3890	0.00262	0.588	0.5143

(1) The concentration of the fluid in contact with the particle surface is equal to the saturated concentration and the controlling resistance to the dissolution of solid is the diffusion through the liquid film surrounding the solid particles.

(2) The velocity distribution and concentration of fluid are uniform at any cross-section of the test section.

(3) The specific surface of the particles in each bed is uniform.

(4) Axial turbulent diffusion coefficient, Ez, in each bed rsmains constant under definite flow conditions.

(5) The process is isothermal.

Under those assumptions and the boundary conditions, the following material balance could be obtained for any bed height, dl:

$$U_o \frac{dC}{dL} = E_z \frac{d^2C}{dl^2} + k_p a(C_s - C) \qquad (31)$$

whers U_o = superficial fluid velocity based on empty column.

C = concentration

C_s = saturated concentration

L = axial distance

E_z = turbulent diffusion coefficient in axial direction, based on bed cross section

kp = particle to fluid mass transfer coefficient

a = specific surface of particles in bed

Assuming that longitudinal or axial mixing in the bed can be negligible:

$$E_z \frac{d^2C}{dl^2} = 0 \qquad (32)$$

Then, equation (31) can be expressed as:

$$U_o \frac{dC}{dL} = k_p\, a(C_s - C) \tag{33}$$

By integration of the equation (33)

$$U_o \int_{C_o}^{C_1} \frac{dC}{C_s - C} + U_o \int_{C_1}^{C_2} \frac{dC}{C_s - C} = (k_p)_f\ a_f \int_o^{L_1} dL + (k_p)_{pa}\, a_{pa} \int_{L_1}^{L_2} dL \tag{34}$$

$$\text{or}\quad U_o \ln \frac{C_s - C_o}{C_s - C_1} + U_o \ln \frac{C_s - C_1}{C_s - C_2} = (k_p)_f\, a_f\, h_f + (kp)_{pa}\, a_{pa}\, h_{pa} \tag{35}$$

where Co = inlet concentration $\left[M/L^3 \right]$

C_1 = concentration of the interface between the fixed and fluidized bed $\left[M/L^3 \right]$

C_2 = outlet concentration $\left[M/L^3 \right]$

$(k_p)f$ = mass transfer coefficient in fluidized bed $\left[L/\theta \right]$

$(k_p)_{pa}$ = mass transfer coefficient in packed bed $\left[L/\theta \right]$

a_f = specific surface of particles in fluidized bed $\left[L^{-1} \right]$

a_{pa} = specific surface of particles in packed bed $\left[L^{-1} \right]$

h_f = height of fluidized bed $\left[L \right]$

h_{pa} = height of fixed bed $\left[L \right]$

h = total height = $h_f + h_{pa}$ $\left[L \right]$

Equation (35) can be further simplified as:

$$U_o \ln \frac{C_s - C_o}{C_s - C_2} = (kp)_f\, a_f\, h_f + (kp)_{p_a}\, a_{p_a}\, hpa \tag{36}$$

If the weighted mean value of $k_p a$ based on the overall bed height is defined as:

$$(k_p)_m\, a_m = (k_p)_f\, a_f \frac{h_f}{h} + (k_p)_{pa}\, a_{pa} \frac{h_{pa}}{h} \tag{37}$$

Then equation (36) may be transformed into the following form:

$$U_o \ln \frac{C_s - C_o}{C_s - C_2} = (k_p)_m\, a_m\, h \tag{38}$$

where $(a)_m$ = overall mean specific surface of particles in bed

$(kp)_m$ = overall mean mass transfer coefficient

Since

$$(\Delta C)_{lm} = \frac{C_2 - C_o}{\ln \frac{C_s - C_o}{C_s - C_2}} \tag{39}$$

$$\text{or} \quad \ln \frac{C_s - C_o}{C_s - C_2} = \frac{C_2 - C_o}{(\Delta C)_{lm}} \tag{40}$$

$$\frac{U_o (C_2 - C_o)}{(\Delta C)_{lm}} = (k_p)_m\, a_m h \tag{41}$$

Then, the overall mean mass transfer coefficient can be calculated as

$$(kp)_m = \frac{U_o(C_2 - C_o)}{a_m h\, (\Delta C)_{lm}} \tag{42}$$

or, by multiplying both sides of the equation by ρ, the above equation can be further transformed into the form:

$$(k_L)_m = \frac{G'(C_2 - C_o)}{A(\Delta C)_{lm}} \tag{43}$$

where $(k_L)_m$ = overall mean mass transfer coefficient $\left[M/L^2\theta\right]$

G' = flow rate through bed $\left[M/\theta\right]$

C_2, C_o = inlet and outlet concentration $\left[M/M\right]$

A = total particle surface in bed $\left[L^2\right]$

In order to account for the effect of axial mixing, which was neglected previously, a correction factor (6), F, to modify the logarithmic mean driving potential can be introduced as:

$$(k_L)_m = \frac{G'(C_2 - C_o)}{A(\Delta C)_{l.m}F} \tag{44}$$

or $$(k_L)_m F = \frac{G'(C_2 - C_o)}{A(\Delta C)_{lm}} \tag{45}$$

In case the axial concentration gradient is available, the value of k_L in each bed can be directly calculated from the definition of k_L by use of the integrated mean driving force as:

$$(k_L)_f = \frac{G'(C_1 - C_o)}{A_f(\Delta C)_{tf.}} \tag{46}$$

$$(k_L)_{Pa} = \frac{G'(C_2 - C_1)}{A_p(\Delta C)_{tp.}} \tag{47}$$

or the overall mean mass transfer coefficient may be evaluated as

$$(k_L)_m = \frac{G'(C_2 - C_o)}{A(\Delta C)_{t.m}}$$

$$= \frac{G'(C_2 - C_1) + G(C_1 - C_o)}{A(\Delta C)_{t.m.}}$$

$$= \frac{(k_L)_{Pa} A_p (\Delta C)_{t.p.} + (k_L)_f A_f (\Delta C)_{tf.}}{A(\Delta C)_{t.m}}$$

$$= X(k_L)_{Pa} \frac{(\Delta C)_{t.p.}}{(\Delta C)_{t.m.}} + (1 - X)(k_L)_f \frac{(\Delta C)_{t.f.}}{(\Delta C)_{t.m}} \tag{48}$$

where $X = \frac{A_p}{A}$, surface fraction of fixed bed particles or weight fraction of packed bed.

A dimensionless parameter, the j_d factor, was first defined by Chilton and Colburn (3) for the purpose of correlating the transfer coefficient k_L to the physical properties of the system. For dilute solution, j_d factor is defined as (3):

$$J_d = \frac{k_L}{G}(N_{Sc})^{\frac{2}{3}} \tag{49}$$

Another dimensionless parameter, the Sherwood number, has also been frequently utilized to correlate the mass transfer data. It is defined as (30) (32) (33):

$$N_{sh} = \frac{k_p D_p}{D_v} \tag{50}$$

As described already, in semi-fluidization, the overall porosity, ϵ, can be arbitrary controlled by adjusting the moveable top sieve plate, and, therefore, it should be considered as an independent variable rather than dependent variable.

In general

$$J_d = f(N'_{Re}, \epsilon) \tag{51}$$

or

$$N_{sh} = f(N'_{Re}, N_{Sc}, \epsilon) \tag{52}$$

for the mass transfer between the solid and fluid phases flowing through the bed of solid particles.

RESULTS OF EXPERIMENT

In the first series of experiments, measurements included the following variables: exit concentration, water temperature, water flow rate, bed depth, top sieve plate height, and particle and bed

characteristics. Computed variables derived from these measurements included k_L, J_d, N'_{Re}, N_{Sh}, N_{Sc}, ϵ and J'_d.

The range of major variables were as follows:

Particle diameter: 8-10 mesh, 12-14 mesh, and 20-24 mesh.

Water temperature: 16.8 C to 24 C.

Bed depth: 3 in. to 6 in.

Voidage: 0.65 to 0.90

Modified Reynolds number: 5 to 130

Sherwood number: 21 to 116

Schmidt number: 1020 to 1540

They are tabulated in Table 2 in the appendix.

Table 3 in the appendix contains the measured and derived data for the second series of experiments in which the axial concentration gradients of fluid were measured in addition to those variables mentioned above.

All the recalculated values for Evan and Gerald's (8) data are tabulated in Tables 4 and 5 in the appendix.

Concentration gradients measured in the second series of experiments are all graphically illustrated in the appendix.

CORRELATION OF RESULTS

First, the mass transfer data were correlated in terms of the J_d factor and modified Reynolds number as is illustrated in Plate X. The mass transfer coefficients were calculated on the basis of the overall logarithmic mean driving force, as was done by other investigators (4) (8) for the packed and fluidized bed mass transfer.

As defined previously, the J_d factor for the dilute solutions is written as (28):

$$J_d = \frac{k_L}{G} (N_{Sc})^{2/3} = (N_{Sh})(N'_{Re})^{-1}(N_{Sc})^{-1/3} \qquad (53)$$

As discussed previously in this investigation, instead of $(k_L)_m$, $(k_L)_m F$ was employed not only to show the existence of the axial mixing effect but also to indicate the use of the overall logarithmic mean driving concentration including both the packed and fluidized bed.

The broken line in Plate X represents the generalized correlation used by Chu, et al., (4) to correlate the mass transfer data in both packed and fluidized beds. The solid line correlates all the semi-fluidized data with the magnitude of the deviations comparable to the correlation used by Chu, et. al. (4). The equation for the solid line was found to be:

$$J_d = 1.865 \left(\frac{N'_{Re}}{1-\epsilon}\right)^{-0.48} \qquad (54)$$

Under convective conditions, either natural or forced, a relationship for mass transfer similar to that obtained for heat transfer may be expected to have a form (16):

$$N_{sh} = f(N'_{Re}, N_{Sc}, N'_{Gr}) \qquad (55)$$

where N_{Sh}, N'_{Re}, N_{Sc}, and N'_{Gr} are respectively the Sherwood, Reynolds, Schmidt and Grashof number for the mass transfer. Such relationship has been obtained theoretically by Eckert (5) (16) from a consideration of the boundary condition.

For mass transfer under the condition of forced convection where the Grashof number is unimportant, the general expression becomes:

EXPLANATION OF PLATE X

J_d factor vs. $N'_{Re}/(1-\epsilon)$ correlation of first series data by use of logarithmic mean driving force.

Ordinate: J_d, dimensionless

Abscissa: $N'_{Re}/(1-\epsilon)$, dimensionless

Legend:

_____ Correlation line of author's data

__ __ __ __ __ Chu and other (4) correlation line

___ _ ___ _ ___ Correlation line of Evan and Gerald's data (8)

○ 8-10 mesh particle

● 12-14 mesh particle

△ 20-24 mesh particle

PLATE X

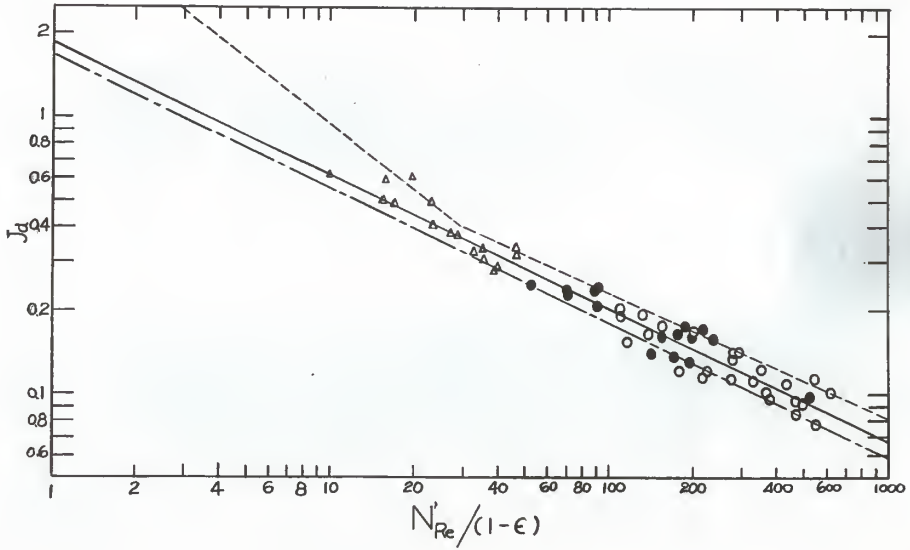
2
1
0.8
0.6
0.4
0.2
0.1
0.08
0.06
J_d
1
2
4
6
8
10
20
40
60
80
100
200
400
600
1000
$N'_{Re}/(1-\epsilon)$

$$N_{Sh} = f\,(N'_{Re},\ N_{Sc}) \tag{56}$$

which boundary layer theory euggeste, should take the form: (5)

$$N_{Sh} \propto N'^{1/2}_{Re}\ N_{Sc}^{1/3} \tag{57}$$

Froseling (11) and Garner and Suckling (16) from the study of the mass tranefer from a single epherical particle in fluids derived a relationehip which may be written in the form:

$$N_{Sh} = 2.0 + aN'^{1/2}_{Re}\ N_{Sc}^{1/3} \tag{58}$$

Fuchs (12) ehowed theoretically that the limiting value of the dimensionless maee transfer Sherwood number is 2.0, which appears in the right hand side of the equation, when the sphere become infinitely small.

Ae already reviewed in the previoue chapter, Shirai (30) derived a similar equation for a generalized correlation of mass tranefer including packed beds, fluidized beds, and eingle spheree into one single line. Shirai's correlation ie written as:

$$N_{Sh\,\epsilon} = 2.0 + 0.75\ N'^{1/2}_{Re} N_{Sc}^{1/3} \tag{59}$$

Plate XI showe the eimilar correlation for the present data and a comparison with Shirai'e equation (30). The best line through the data is expressed as:

$$N_{Sh\,\epsilon} = 2.0 + 0.46 N'^{0.543}_{Re}\ N_{Sc}^{0.33} \tag{60}$$

Since the J_d factor correlation was derived primarily for turbulent condition, no allowance is made for the effect of transfer by natural convection and the molecular diffusion. According to the Chu et al., (4)

EXPLANATION OF PLATE XI

$\frac{N_{Sh\epsilon}\ -2}{N_{Sc}^{1/3}}$ vs. N'_{Re} correlation of first series data by use of logarithmic mean driving force.

Ordinate: $\frac{N_{Sh\epsilon}\ -2}{N_{Sc}^{1/3}}$, dimensionless

Abscissa: N'_{Re}, dimensionless

Legend:

_____ Correlation line of author's data

_ _ _ _ _ _ _ _ _ Shirai's (30) correlation line

__ - __ - __ - __ - __ Correlation line of Evan and Gerald's data (8)

○ 8-10 mesh particle

● 12-14 mesh particle

△ 20-24 mesh particle

PLATE XI

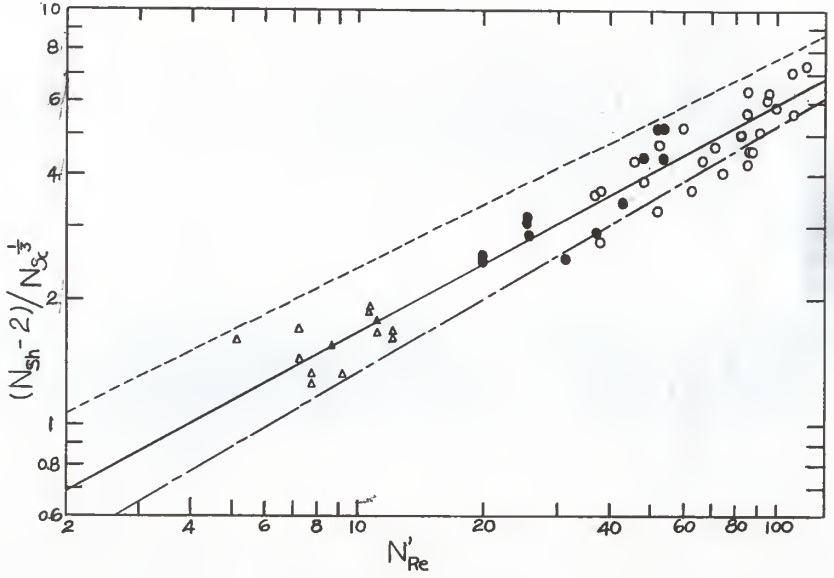

the J_d factor correlation can be generally expressed as a function of the Reynolds number as:

$$J_d = \frac{k_L}{G} (N_{Sc})^{2/3} = a\left(\frac{N'_{Re}}{1-\epsilon}\right)^{-b} \qquad (61)$$

or, in terms of the Sherwood number it is written as:

$$N_{sh} = a(N'_{Re})^{1-b} (N_{Sc})^{1/3} (1-\epsilon)^{b} \qquad (61')$$

The equation above can be modified by an analogical method used by previous investigators (12) (30) (32) (33) to account for the molecular diffusion at low Reynolds number as follows:

$$N_{sh} = 2.0 \quad a (N'_{Re})^{1-b} (N_{Sc})^{1/3} (1 - \epsilon)^{b} \qquad (62)$$

Then, a modified J_d factor, J'_d, may be defined as:

$$Jd' = \frac{N_{sh} - 2}{(N'_{Re})(N_{Sc})^{1/3}}$$

Plate XII shows the plot of jd' vs $\frac{N'_{Re}}{1-}$, which yields the relationship:

$$J_d' = 1.51 \left(\frac{N'_{Re}}{1-\epsilon}\right)^{1/2} \qquad (64)$$

or $$N_{sh} = 2.0 + 1.51 \left[N'_{Re}(1 - \epsilon) \right]^{1/2} \left[N_{Sc} \right]^{1/3} \qquad (65)$$

The correlations for the second series of the experiments, which are similar to the ones described above, are plotted in Plates XIII, XIV, and XV.

EXPLANATION OF PLATE XII

J'_d vs. $N'_{Re}/(1-\epsilon)$ correlation of first series data by use of logarithmic mean driving force

Ordinate: J'_d, modified Jd factor, dimensionless

Abscissa: $N'_{Re}/(1-\epsilon)$, dimensionless

Legend:

_____ Correlation line of author's data

__ – __ – __ – __ – __ Correlation line of Evan and Gerald's data (8)

○ 8-10 mesh particle

● 12-14 mesh particle

Δ 20-24 mesh particle

PLATE XII

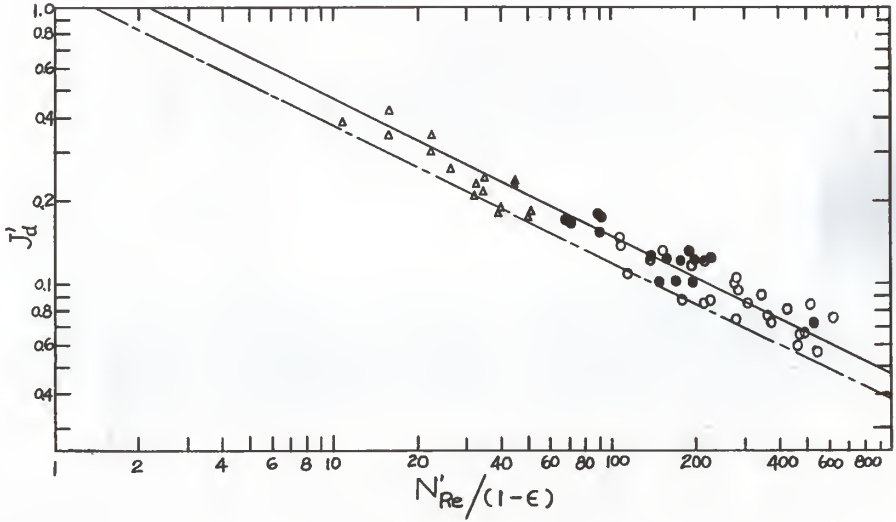
1.0
0.8
0.6
0.4
0.2
0.1
0.08
0.06
0.04
J'_d
1
2
4
6
8
10
20
40
60
80
100
200
400
600
800
$N'_{Re}/(1-\epsilon)$

EXPIANATION OF PLATE XIII

Jd factor vs. $N'_{Re}/(1-\epsilon)$ correlation of second series data by use of integrated mean driving force

Ordinate: Jd, dimensionless

Abscissa: $N'_{Re}/(1-\epsilon)$, dimensionless

Legend:

_____ Line of equation (54)

○ 8-10 mesh particle

● 12-14 mesh particle

Δ 20-24 mesh particle

PLATE XIII

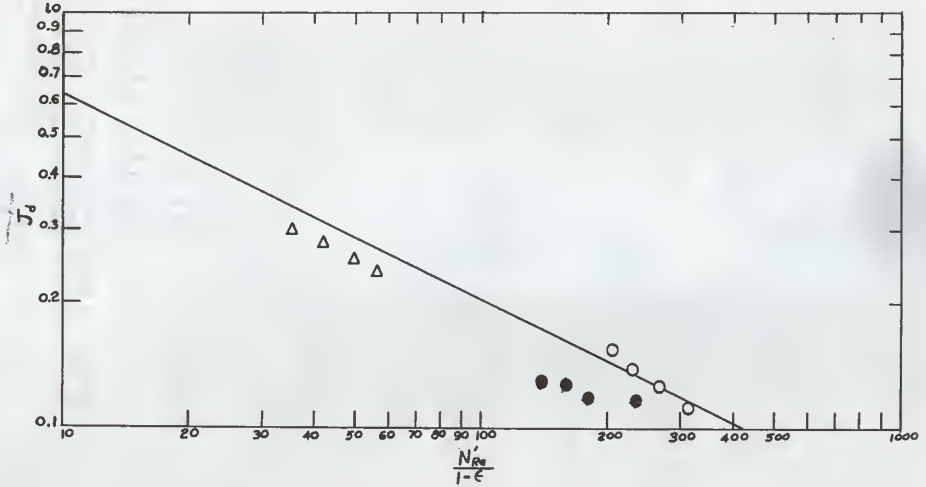
1.0
0.9
0.8
0.7
0.6
0.5
0.4
0.3
0.2
0.1
J_d
10
20
30
40
50
60
70
80
90
100
200
300
400
500
1000
$\frac{N'_{Re}}{1-\epsilon}$

EXPLANATION OF PLATE XIV

$(N_{sh\epsilon} - 2)/N_{Sc}^{1/3}$ vs. N'_{Re} correlation of second series data by use of integrated mean driving force

Ordinate: $(N_{sh\epsilon} - 2)/N_{Sc}^{1/3}$, dimensionless

Abscissa: N'_{Re}, dimensionless

Legend:

———————————— Line of equation (60)

O 8-10 mesh particle

● 12-14 mesh particle

Δ 20-24 mesh particle

PLATE XIV

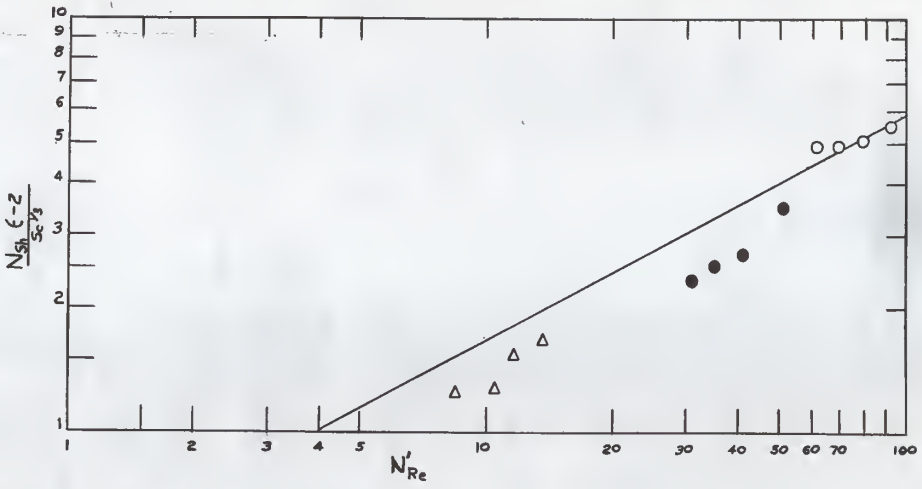
$\frac{N_{Sh}\,\epsilon - 2}{Sc^{1/3}}$
N'_{Re}
10
9
8
7
6
5
4
3
2
1
1
2
3
4
5
10
20
30
40
50
60
70
100

EXPLANATION OF PLATE XV

J'_d vs. $N'_{Re}/(1-\epsilon)$ correlation of second series data by use of integrated mean driving force

Ordinate: J'_d, modified Jd factor, dimensionless

Abscissa: $N'_{Re}/(1-\epsilon)$, dimensionless

Legend:

———————— Line of equation (65)

○ 8-10 mesh particle

● 12-14 mesh particle

Δ 20-24 mesh particle

PLATE XV

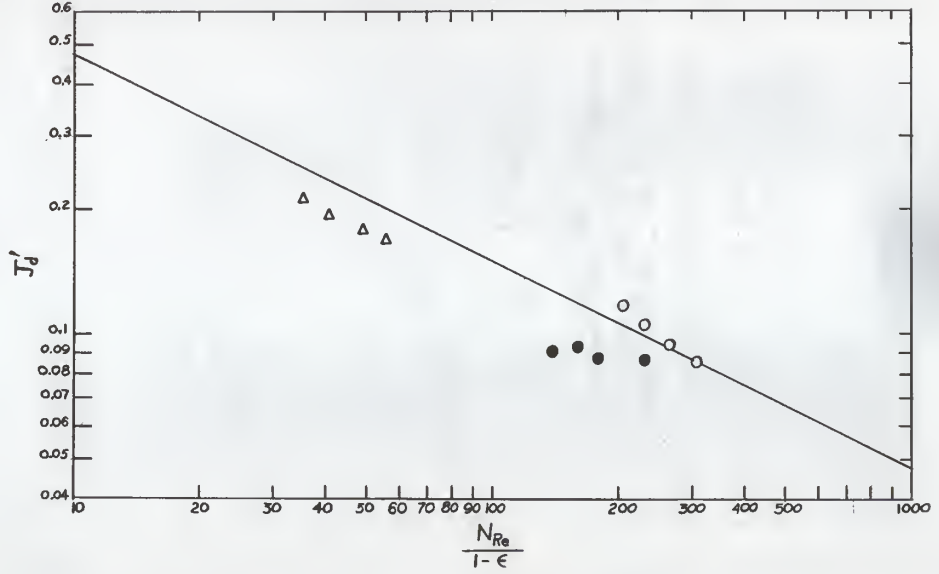
0.6
0.5
0.4
0.3
0.2
0.1
0.09
0.08
0.07
0.06
0.05
0.04
J_d'
10
20
30
40
50
60
70
80
90
100
200
300
400
500
1000
$\frac{N_{Re}}{1-\epsilon}$

DISCUSSION

In order to intelligently understand the effect of the packed bed formation on the mass transfer in the fluidized bed, the mechaniem of the packed bed formation should be understood first. At least the size of the packed bed should be quantitatively correlated with the independent variables of the experiment and the characteristice of ordinary fluidization under eimilar flow conditions.

The experimental data of the present investigation, as ehown in Platee XVI, XVII and XVIII, definitely indicate that the segregation of the particlee depende on factore such as the particle and fluid characterietice, flow conditione and the expansion of the bed.

Baeed on a simple material balance, the height of the packed bed eection in a eemi-fluidized bed can be derived as follows (9) (10). It is assumed that the liquid is incompressible, the particlee in a column do not interact with each other and the particle distribution ie uniform. Referring to Plate XIX:

$$h_{pa}\rho_s (1 - \epsilon_{pa}) = \left[h_{pa} + (h_{fo} - h) \right] \rho_s (1 - \epsilon_f) \qquad (66)$$

or

$$h_{pa} = (h_{fo} - h) \left(\frac{1 - \epsilon_f}{\epsilon_f - \epsilon_{pa}} \right) \qquad (67)$$

where h_{pa} = height of packed bed section

ϵ_{pa} = poroeity of the packed bed eection

h_{fo} = height of the bed under complete fluidization conditions

ϵ_f = poroeity of the fluidized bed section

h = height of the top eieve plate

EXPLANATION OF PLATE XVI

Weight fraction of packed particles

Particle size: 8-10 mesh

Ordinate: X, Weight fraction in packed bed, dimensionless

Abscissa: G, Fluid rate, lb/(hr.) (sq. ft.)

PLATE XVI

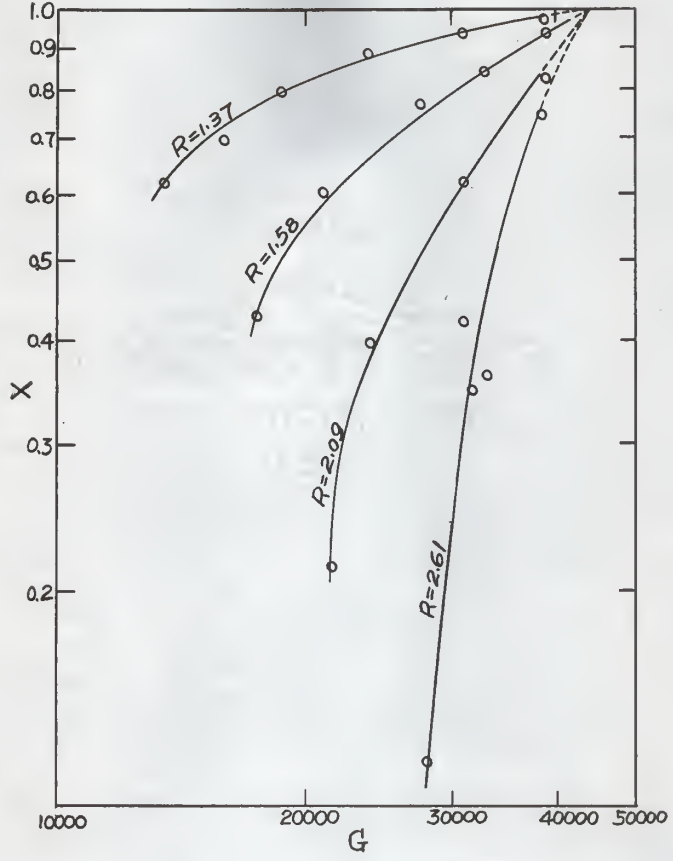
1.0
0.9
0.8
0.7
0.6
0.5
0.4
0.3
0.2
X
R=1.37
R=1.58
R=2.09
R=2.61
10000
20000
30000
40000
50000
G

EXPLANATION OF PLATE XVII

Weight fraction of packed particles

Particle size: 12-14 mesh

Ordinate: X, Weight fraction in packed bed, dimensionless

Abscissa: G, Fluid rate, lb./(hr.)(sq. ft.)

PLATE XVII

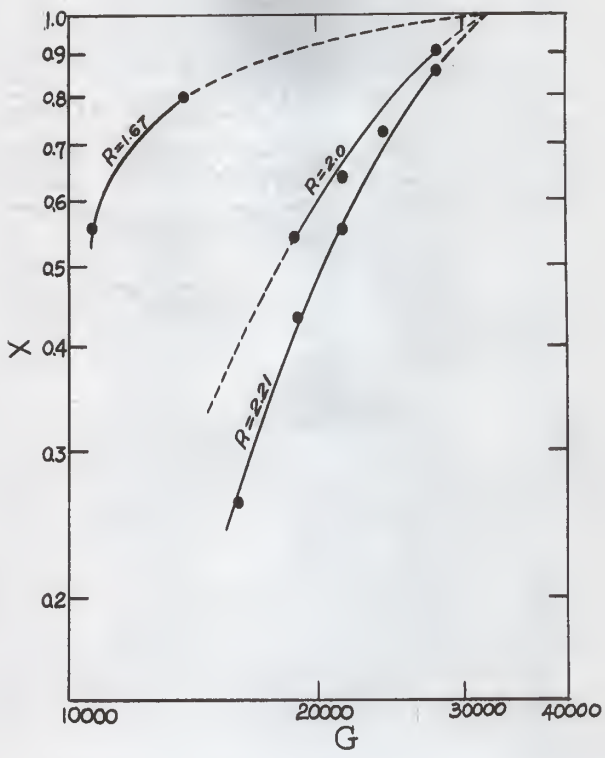
1.0
0.9
0.8
0.7
0.6
0.5
X 0.4
0.3
0.2
1
T
R=1.67
R=2.0
R=2.21
10000
20000
30000
40000
G

EXPLANATION OF PLATE XVIII

Weight fraction of packed particles

Particle size: 20-24 mesh

Ordinate: X, Weight fraction in packed bed, dimensionless

Abscissa: G, Fluid rate, lb./(hr.)(sq. ft.)

PLATE XVIII

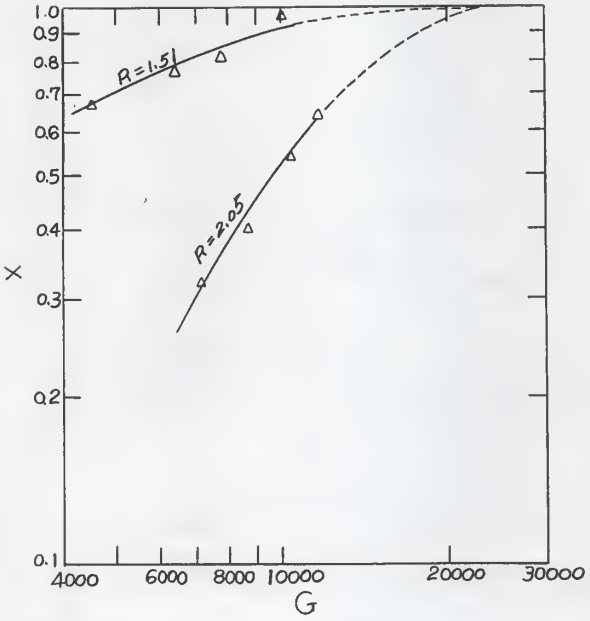
1.0
0.9
0.8
0.7
0.6
0.5
0.4
0.3
0.2
0.1
X
R=1.51
R=2.05
4000
6000
8000
10000
20000
30000
G

EXPLANATION OF PLATE XIX

Schematic diagram of semi-fluidized bed

PLATE XIX

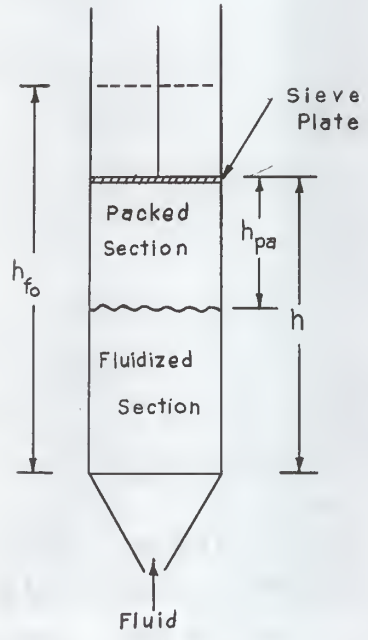
Sieve
Plate
Packed
Section
h_{pa}
h_{fo}
h
Fluidized
Section
Fluid

In the right hand side of the above equationa, h and ϵ_{pa} are independent variablss of the experiment. The relationship between h_f or ϵ_f and flow conditions can be obtained from the Evan and Gerald'e data (8). The height of the packed bed saction calculated from equation (67) and that obtained from the experimente are compared ae ehown in Plate XX.

The weight fraction of solid in the packed bed aection, X, then, can bs calculated as:

$$X = \rho_a \cdot A \cdot h_{pa}(1 - \epsilon_{pa})/W$$

$$= \frac{\rho_e A(1 - \epsilon_{pa})(h_{fo}-h)\ (1 - \epsilon_f)}{W \qquad (\epsilon_f - \epsilon_{pa})} \qquad (68)$$

The experimental data are compared with the calculated valuea based on the equation (68) aa ahown in Plate XXI.

The agreement indicated in Plate XX and Plate XXI is good conaidering the fact that the large and irregular eize particles of benzoic acid were employed and that the data in the range of $\epsilon > 0.8$ were not accurate due to ths difficulty of meaeurement of bed height (8) (9) (10).

As indicated in the figuree the deviation for the larger particlea ie greater than that for the smaller ones. The errore were probably due to ths difficulty in meaeuring the expanded heighta of fluidized beds of the coarse and the irregular particlee, and the aseumption of uniform bed density.

It is alao intsresting to note that the extrapolated curvss of X vs. G for each partiole sizes all converge to one value of G at X = 1 and these values of G coincide with the value of G at $\epsilon_f = 1$ obtained from

EXPLANATION OF PLATE XX

Heights of packed bed section calculated based on equation (67) compared with that experimentally observed

Ordinate: h_{pa}, Observed height, ft.

Abscissa: h_{pa}, Calculated height, ft.

PLATE XX

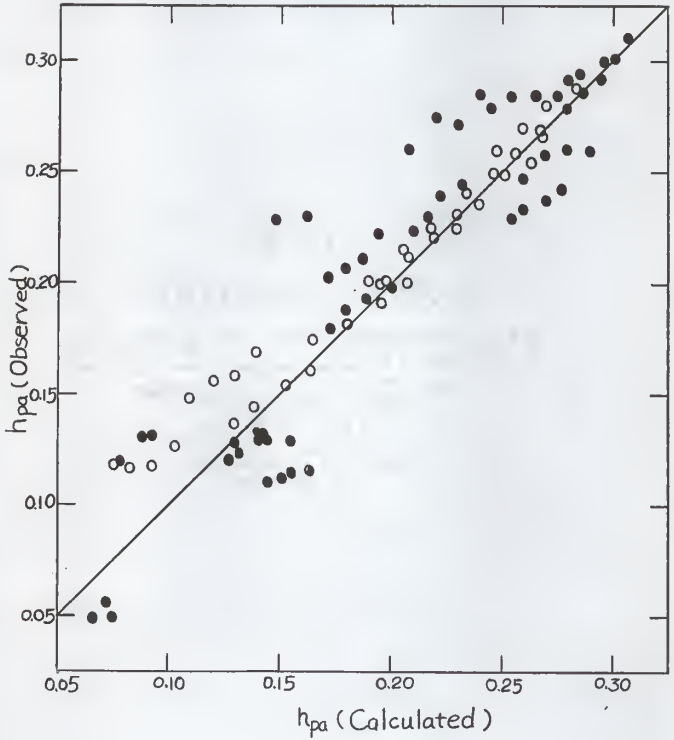
0.30
0.25
0.20
0.15
0.10
0.05
h_{pa} (Observed)
0.05
0.10
0.15
0.20
0.25
0.30
h_{pa} (Calculated)

EXPLANATION OF PLATE XXI

Weight fraction of packed bed section calculated based on equation (68) compared with that experimentally measured

Ordinate: X, Weight fraction measured, dimensionless

Abscissa: X, Weight fraction calculated, dimensionless

PLATE XXI

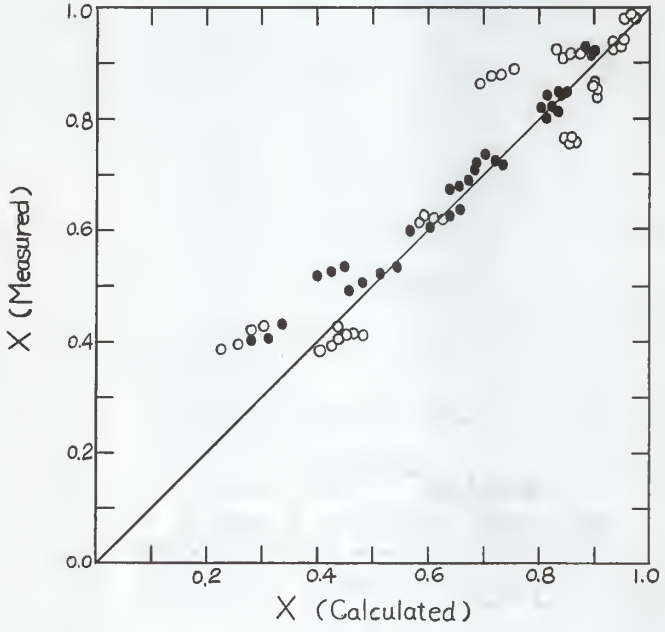

the extrapolation of the curve of ϵ_f vs. G as shown in Plate II. Theoretically, all the particles in the fluidized bed disappear, or in the other words, when X becomes unity the fluid flow rate reaches the maximum fluid velocity at which $\epsilon_f = 1$.

Chu and co-workers (4) have pointed out that the experimental error is effected by the degree of saturation of the outlet solution. The experimental errors are magnified by a factor of 4 at 90% saturation when used to compute the mass transfer coefficient and after 90% saturation the degree of multiplication of experimental errors increase sharply, which makes precise measurements in this region quite difficult. Now, referring to Plate X, it may be seen that Chu's original J_d factor correlation yields j_d values consistently higher than the present experimental data. Chu's correlation was derived only for the ordinary fluidized and packed beds and the maximum deviation of his correlation appears to be 22% in the range of Reynolds numbers used in the present experiments. Furthermore, Evan and Gerald's (8) data for benzoic acid-water system were not included in the original correlation by Chu et. al. (4). Evan and Gerald's (8) data were recalculated in terms of J_d vs. $\frac{N'Re}{1-\epsilon}$.

It clearly indicated that Evan and Gerald's (8) data also deviate consistently from Chu's et al., (4) original correlation with approximately the same magnitudes as those of the semi-fluidized bed data. Their packed bed data are correlated as:

$$J_d = 2.132 \left(\frac{N'Re}{1-\epsilon}\right)^{0.5122} \qquad (69)$$

and the fluidized bed data are correlated as:

$$J_d = 1.340 \left(\frac{N'Re}{1-\epsilon}\right)^{0.4675} \tag{70}$$

Consequently, the overall correlation of Evan and Gerald's (8) data may be expreseed as:

$$J_d = 1.68 \left(\frac{N'Re}{1-\epsilon}\right)^{0.49} \tag{71}$$

Comparison of equations (71) with (54) reveals that, within the range of the variables of the present investigation and the errors of experimentation the semi-fluidized data may be correlated as well as the data for ordinary fluidized and packed beds by use of J_d factor vs. $\frac{N'Re}{1-\epsilon}$, which is based on the overall mean mass transfer coefficient, $(k_L)_m$. As mentioned previously, the J_d factor used in Plate X should include the F factor to indicate that the overall logarithmic mean driving force was used in spite of the existence of axial mixing of the fluid and the abrupt change in the axial concentration gradient.

The data for the benzoic acid-water system were also not included in Shirai's (30) original generalized correlation including the fluidized bed, fixed bed, and a single particle. Evan and Gerald's (8) data were again recorrelated by the method suggested by Shirai (30). It is illustrated in Plate XI and the calculations are summarized in Tables 4 and 5, Appendix.

Plate XI indicates that the experimental data were consistently lower than the calculated values by approximately 38%. However, this is within the range of accuracy expected from the generalized correlation of Shirai

(30) for any specific system. Evan and Gerald's (8) data are expressed as follows:

For packed bed:

$$N_{Sh\epsilon} = 2 + 0.424N'^{0.558}_{Re}N_{Sc}^{1/3} \tag{72}$$

For fluidized bed:

$$N_{Sh\epsilon} = 2 + 0.230N'^{0.659}_{Re}N_{Sc}^{1/3} \tag{73}$$

For overall correlation:

$$N_{Sh\epsilon} = 2 + 0.312N'^{0.608}_{Re}N_{Sc}^{1/3} \tag{74}$$

The overall correlation expressed by equation (74) is again very similar to that for the semi-fluidized data as expressed by equation (65) and Plate XII. These similarities of the correlation between the ordinary packed beds and semi-fluidized beds by use of the methods suggested by Chu et.al.(40) and Shirai (30) would indicate that it is possible, at least for the purpose of approximation to consider the semi-fluidized bed to possess uniform solid density distribution. When correlations are not available for any specific system for semi-fluidization, some form of the generalized mass transfer correlation of the ordinary packed and fluidized beds may be employed to estimate the mean mass transfer coefficients.

Equation (65) which was derived by modification of the J_d factor correlation to the present data yields a mean deviation of 11.7% while equations (54) and (60) give a deviation of 9.87% and 11.73% respectively. This implies that the use of the modified correlation as expressed by equation (65) does not improve the correlation. However, the form of this equation would agree with the expression predicted by the boundary layer theory which is:

$$N_{Sh} \propto N'_{Re}{}^{1/2} N_{Sc}{}^{1/3} \tag{57}$$

In addition, the use of this expression offers much simpler means of calculation.

Evan and Gerald's (8) data were recorrelated in form of equation (65). The packed bed data are correlated as:

$$N_{Sh} = 2 + 1.483 \left[(N'_{Re})(1 - \epsilon) \right]^{1/2} \left[N_{Sc} \right]^{1/3} \tag{75}$$

and the fluidized bed data are correlated as:

$$N_{Sh} = 2 + 1.031 \left[(N'_{Re})(1 - \epsilon) \right]^{1/2} \left[N_{Sc} \right]^{1/3} \tag{76}$$

and overall correlation equation may be expressed as:

$$N_{Sh} = 2 + 1.202 \left[(N'_{Re})(1 - \epsilon) \right]^{1/2} \left[N_{Sc} \right]^{1/3} \tag{77}$$

or as Plate XII indicates:

$$N_{Sh} \simeq 2 + 1.51 \left[(N'_{Re})(1 - \epsilon) \right]^{1/2} \left[N_{Sc} \right]^{1/3} \tag{77'}$$

It is interesting to note that their data of ordinary packed and fluidized beds are well correlated by the same equation as equation (65). However, equation (65) or any other similar mass transfer equation has different significance when applied to the semi-fluidized bed that when applied to the ordinary packed and fluidized beds. As already stated, the overall porosity of the semi-fluidized bed is an independent variable of the experiment, i.e. it can be arbitrarily changed or fixed. It can be expressed as:

$$\epsilon = 1 - \frac{1 - \epsilon_o}{R} = \frac{V - W/\rho_s}{V} = 1 - \frac{W}{\rho_s h S} \tag{78}$$

Where ϵ_o and ρ_s are characteristics of the solid particle and V, h, W, and S are the variables which can be independently determined. Substitution of equation (78) into the equation (65) leads to the following relationship:

$$(k_L)_m F \propto (\frac{1}{R})^{1/2} = R^{-1/2} \tag{79}$$

or

$$(k_L)_m F \propto (\frac{1}{hS})^{1/2} = (hS)^{-1/2} \tag{80}$$

Or for the column with definite cross-section:

$$(k_L)_m F \propto (\frac{1}{h})^{1/2} = (h)^{-1/2} \tag{81}$$

These characteristics of the semi-fluidized bed are illustrated in Plate XXII. In Plate XXII the data at flow rate G = 28,000 lb/(hr)(ft^2) are used.

On the other hand, there is no freedom to alter the porosity of the packed bed in the operation of a particular system, i.e.

$$(k_L)_m F \neq f(\epsilon) \tag{82}$$

or

$$(k_L)_m F \neq f(R \text{ or } h) \tag{83}$$

Equations (54) (60) and (65), when applied to the fluidized bed, cannot be considered as explicit equations, since ϵ is again a function of the flow condition. In order to change ϵ, the flow rate has to be changed.

EXPLANATION OF PLATE XXII

Expansion ratio vs. mass-transfer coefficient

Ordinate: k_L, Mass-transfer coefficient, lb/(hr.)(sq.ft.)

Abscissa: R, expansion ratio, dimension

PLATE XXII

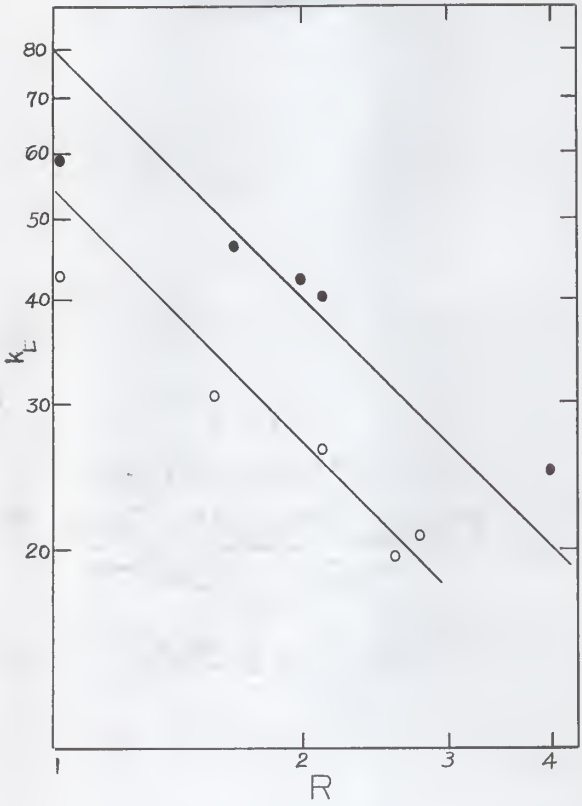

This implies that the F-factors included in the correlation of the data from the first series of the experiments were close to unity, in other words, the effects of axial fluid mixing and the exietence of abrupt change in the axial concentration profile were emall. The valuee of F are plotted against X and $\frac{N'Re}{1-\epsilon}$ in Platee XXIII and XXIV reepectively. The conditions of no axial mixing of fluid and existence of smooth concentration gradient profile lead to the value of F = 1. The maximum deviation as indicated in Plate XXIII and XXIV wae 7.65% and no abrupt change in the axial concentration gradient.

Finally equation (48) developed earlier was tested by use of the experimental data. In Plate XXV, the calculated values are plotted against the experiment values. The validity of equation (48) indicates the internal mechanism of mase transfer in the semi-fluidized bed. It can be described as follows: the overall mass tranefer coefficiente of eemi-fluidized beds represents the linear combination of the effective packed bed maes transfer coefficient and the effective fluidized bed mass transfer coefficient which are defined ae $(k_L)_{pa} \frac{(\Delta C)_{tp}}{(\Delta C)_t}$ and $(k_L)_f \frac{(\Delta C)_{t\cdot f}}{(\Delta C)_t}$ reepectively.

In the first series of experimente the axial concentration was not measured and in the correlation of the data, the F-factor, which was originally introduced by Epetein (6) was employed to indicate the use of the logarithmic mean driving force. The importance of the axial mixing in the solid-liquid contact process has been emphasized by various investigatore recently (8) (9). However, it appeare that, so far, there ie no way to predict exactly the axial mixing coefficient of a particular system

EXPLANATION OF PLATE XXIII

(k_L)l.m./(k_L)t.m. vs. weight fraction in packed bed

Ordinate: (k_L)l.m./(k_L)t.m., dimensionless

Abscissa: X, Weight fraction in packed bed, dimensionless

PLATE XXIII

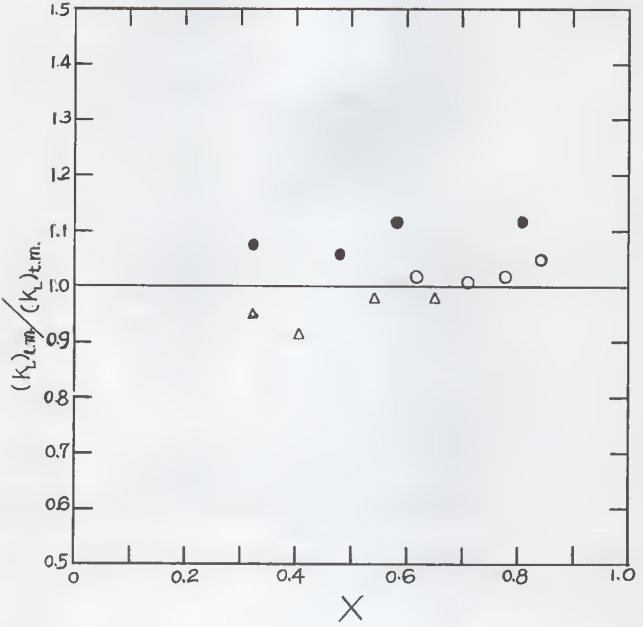

EXPLANATION OF PLATE XXIV

(k_L)l.m./(k_L)t.m. vs. $N'_{Re}/(1 - \epsilon)$

Ordinate: (k_L)l.m./(k_L)t.m., dimensionless

Abscissa: $N'_{Re}/(1 - \epsilon)$

PLATE XXIV

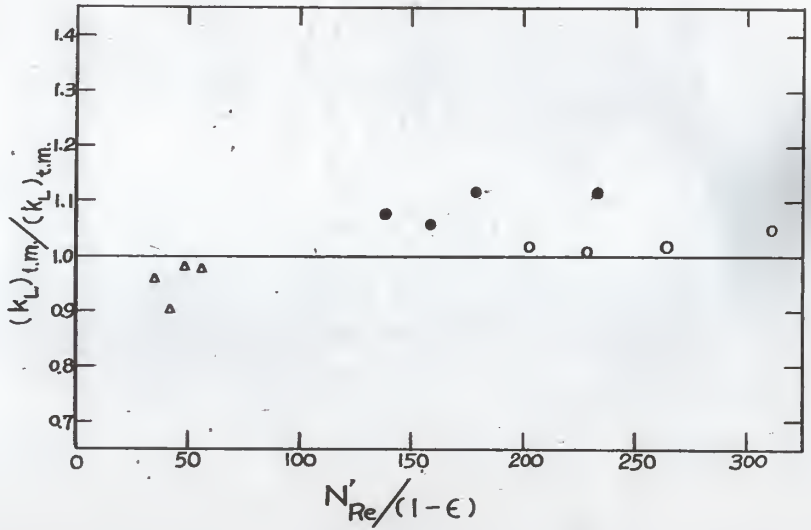
1.4
1.3
1.2
1.1
1.0
0.9
0.8
0.7
$(k_L)_{i.m.}/(k_L)_{t.m.}$
0
50
100
150
200
250
300
$N'_{Re}/(1-\epsilon)$

EXPLANATION OF PLATE XXV

Mass-transfer coefficient calculated based on equation (48)
Compared with that experimentally measured

Ordinate: $(k_L)m$, Measured value, lb./(hr.)(sq.ft.)

Abscissa: $(k_L)m$, Calculated value, lb./(hr.)(sq.ft.)

PLATE XXV

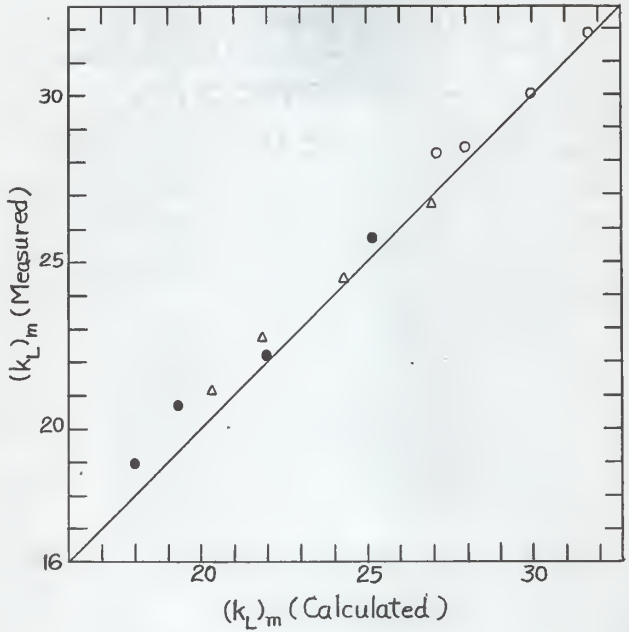

under certain operating conditions with sufficient accuracy for mass transfer calculations. But there is good indication that axial mixing in the liquid-solid systems is much less extensive than in the gas-solid systems especially with large particles such as used in this investigation. Richardson and Mitson (28) studied heat transfer in liquid-solid fluidizing systems and found that the longitudinal temperature gradient throughout the system was only slightly affected by the presence of the solid, indicating that the amount of back mixing of the liquid was negligible.

In Plates XIII, XIV, and XV, the mass transfer coefficients calculated by use of the integrated mean driving force are compared with the correlation obtained in the first series of experiments. They indicate that the deviation of the second series experimental data from the correlation are within the range of the first series of experiments. The use of the integrate of mean driving force eliminated the necessity of F-factor.

CONCLUSION AND SUMMARY

The following significant conclusions could be drawn from the results of the present investigation:

(1) The segregation of the solid particles into two distinct sections, the fixed bed (upper section) and the fluidized bed (lower section) is caused within a single vessel containing the solid particles by denying its full expansion. In other words, it is possible to carry out the fixed bed and fluidized operations simultaneously within a single vessel.

(2) The depth of the packed section, and consequently also the fluidized section, are functions of the flow conditions, particle and fluid characteristics, and the expansion of the bed allowed.

The ratio of the depth of the fixed bed to the depth of the fluidized section can be fixed arbitrarily under certain flow conditions by controlling the expansion of the bed with the upper sieve plate.

(3) The dimensionless equation which correlates the overall mass transfer coefficient of semi-fluidized beds and which is applicable to ordinary packed and fluidized beds was determined.

(4) The rate of mass transfer is also affected, not only by the characteristics of the particles, fluids, and flow rate, but also by the amount of expansion of the bed allowed. The magnitudes of mass transfer coefficients can be controlled in an inverse proportionality to and within the limits of completely fixed bed and a fully fluidized bed by means of bed expansion alone.

(5) The overall mass transfer coefficient of semi-fluidized beds can be evaluated as the linear combination of effective packed bed and fluidized bed mass transfer coefficients.

The expansion of the bed can be introduced as an independent factor, in addition to such factors as temperature, pressure, and flow rate, in controlling the rate of mass transfer for any solid particles-fluid system.

The great possibility of the practical application of this new operation of semi-fluidization is beyond the need of much description from the fact that both fixed beds and fluidized beds are extensively employed in industry as catalystic reactors, ion exchange columns, heat exchangers, driers, solvent extractors, and other process equipment.

It is difficult to predict the occurrence of semi-fluidization for a large diameter column (of the order of 2-3 ft.) based on the evidence from the small laboratory scale column. However, it is believed that such phenomena are quite possible in a particular fluidization, but may not be possible in an aggregative fluidization.

TABLE OF NOMENCLATURE

A = total particle surface area, sq. ft.

C = concentration of benzoic acid in water stream, lb/lb

C_S = concentration of benzoic acid in saturated solution, lb/lb

D_p = equivalent spherical particle diameter, ft.

D_v = diffusivity of benzoic acid in water, (sq.ft.)/hr

F = correction factor, dimensionlees

G = superficial mass velocity, lb/(hr)(sq.ft.)(unit C)

G' = mass velocity, lb/hr

h = height of the top sieve plate or overall depth of bed, ft.

h_o = depth of height of initial bed, ft

h_f = height of fluidized bed section, ft

h_{pa} = height of packed bed section, ft

J_d = mass transfer factor, dimensionless

J'_d = modified mass transfer factor, dimensionless

k_L = mass transfer coefficient, lb/(hr)(sq.ft.)(unit C)

N'_{Gr} = graph of number for mass transfer, dimensionless

N'_{Re} = modified Reynolde number, dimensionless

N_{Sc} = Schmidt number, dimensionlese

N_{Sh} = Sherwood number, dimeneionless

R = bed expansion ratio, dimensionless

S = cross-eection area of the column, sq. ft.

T = temperature, ^oC

V = overall volume of the bed, cu.ft.

W = weight of the particle bed, lb.

X = weight fraction of particles in the packed bed eection, dimensionleee

Greek Letters

ϵ = void fraction or porosity in the bed, dimensionlese

ρ = fluid density, lb/cu. ft.

ρ_B = bulk deneity of the solid, lb/cu. ft.

ρ_S = solid density, lb/cu. ft.

μ = viscosity, lb/(hr)(ft)

ϕ = particle shape factor, dimeneionless

Subscript

f = fluidized bed

p = particle

pa = packed bed

0 = at bed inlet

1 = at interface between packed and fluidized beds

2 = at bed outlet

m = mean value

l.m. = logarithmic mean value

t.m. = integrated mean value

ACKNOWLEDGMENT

The author takes this opportunity to express his appreciation to:

Dr. Henry T. Ward, Head of the Department, for his advice and encouragement.

Dr. L. T. Fan, who originated this study, for his interest and guidance during the work. This appreciation is acknowledged with utmost sincerity for his enthusiastic spirit and wide scope of knowledge in this field have been major factors in the successful fulfillment of this contribution.

The author also wishes to express his gratitude to the Kansas State University Engineering Experiment Station for the financial support.

BIBLIOGRAPHY

1. Carman, P. C.
Soc. Chem. Ind. 57, 225 (1938)

2. Chang, S.
"Determination of Diffusion Coefficients in Aqueous Solutions"
M. S. Thesis, Chem. Engg., M.I.T. (1948)

3. Chilton, T. H. and A. P. Colburn
Ind. Eng. Chem., 26, 1183, (1934)

4. Chu, J. C., J. Kalil, and W. A. Wettereth
Chem. Eng. Progr. 49, 141, (1953)

5. Eckert, E. R. G.
'Introduction to Heat and Mass Transfer',
McGraw-Hill Book Co. Inc., New York, 1950

6. Epstein, N.
The Canadian Journal of Chem. Eng., 36, 210, (1958)

7. Ergun, E.
Chem. Eng. Progr., 48, 228 (1952)

8. Evans, G. C. and C. F. Gerald
Chem. Eng. Progr. 49, 135 (1953)

9. Fan, L. T.
Unpublished note on Semi-fluidization (1953)

10. Fan, L. T., Y. C. Yang and C. Y. Wen
Communication submitted to A.I.Ch.E. Journal (Accepted for publication (1959)

11. Frossling, N.
Gerl. Beit. Zur. Geophysik., 52, 170 (1938)

12. Fuchs, N.
J. Phys. (U. S. S. R.), 6, 224 (1934)

13. Gaffney, B. J. and T. B. Drew
Ind. Eng. Chem. 42, 1120 (1950)

14. Galloway, L. R., W. Komarnicky, and N. Epstein
The Canadian Journal of Chem. Eng., 35, 139 (1957)

15. Gamson, B. W., G. Thodos, and O. A. Hougen
Trans. Am. Inst. Chem. Eng., 39, 1, (1943)

16. Garner, F. H. and R. D. Suckling
A.I.Ch.E. Journal, Vol. 4, No. 1, 115 (1958)

17. Hobson, M. and G. Thodos
Chem. Eng. Progr., 45, 517 (1949)

18. Hurt, D. M.
Ind. Eng. Chem., 35, 522, (1943)

19. International Critical table
McGraw-Hill Book Co. Inc. (1926)

20. Ishine, T., T. Otake, and T. Okada
Chem. Eng. (Japan), 15, 255 (1951)

21. Lemlich, R. and I. Caldes
A.I.Ch.E. Journal, Vol. 4, No. 3, 376 (1958)

22. Linten, W. H. Jr. and T. K. Sherwood
Chem. Eng. Progr. 46, 259 (19)

23. McCune, L. K. and R. H. Welhelm
Ind. Eng. Chem. 41, 1124 (1949)

24. Morse, R. D.
Ind. Eng. Chem. 41, 1117, (1949)

25. Othmer, D. F.
"Fluidization" Reinhold Publishing Corporation, New York, (1956)

26. Perry, J. H.
Chemical Engineers' handbook, 3rd edition
New York, McGraw-Hill Co. (1950)

27. Resnick, W. and R. R. White
Chem. Eng. Progr., 45, 377 (1949)

28. Richerdson, J. F. and A. E. Mitson
Trans. Inst. Chem. Eng. 36, 270 (1958)

29. Seidell, A.
'Solubility of Organic Compounds' 3rd Ed., New York, D. Van
Nostrand Co. (1941)

30. Shirai, T.
Doctor thesis, Tokyo Inst. Tech. (1955)

31. Taecker, R. G. and O. A. Hougen
Chem. Eng. Progr., 45, 188 (1949)

32. Wakao, N., Oshima and Yagi
Chem. Eng. (Japan), 22, 24 (1958)

33. Wakao, N., Oshima and Yagi
Chem. Eng. (Japan), 22, 30 (1958)

34. Wilke, C. R. and O. A. Hougen
Trans. Am. Inst. Chem. Eng., 41, 445 (1945)

APPENDIX

EXPLANATION OF PLATE XXVI

Concentration gradient in a semi-fluidized bed of benzoic acid-water system

Particle size: 8-10 mesh

Ordinate: C, Concentration, lb./lb.

Abscissa: A, Total particle surface, sq. ft.

PLATE XXVI

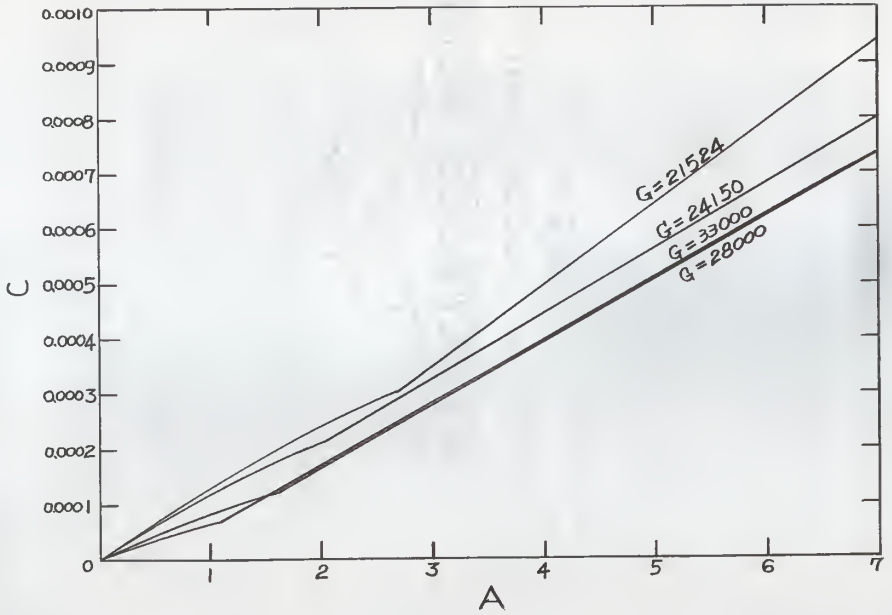
0.0010
0.0009
0.0008
0.0007
0.0006
0.0005
0.0004
0.0003
0.0002
0.0001
0
C
1
2
3
4
5
6
7
A
G=21584
G=24150
G=33000
G=28000

EXPLANATION OF PLATE XXVII

Concentration gradient in semi-fluidized bed of benzoic acid-water system

Particle size: 12-14 mesh

Ordinate: C, Concentration, lb./lb.

Abscissa: A, Total particle surface, sq. ft.

PLATE. XXVII

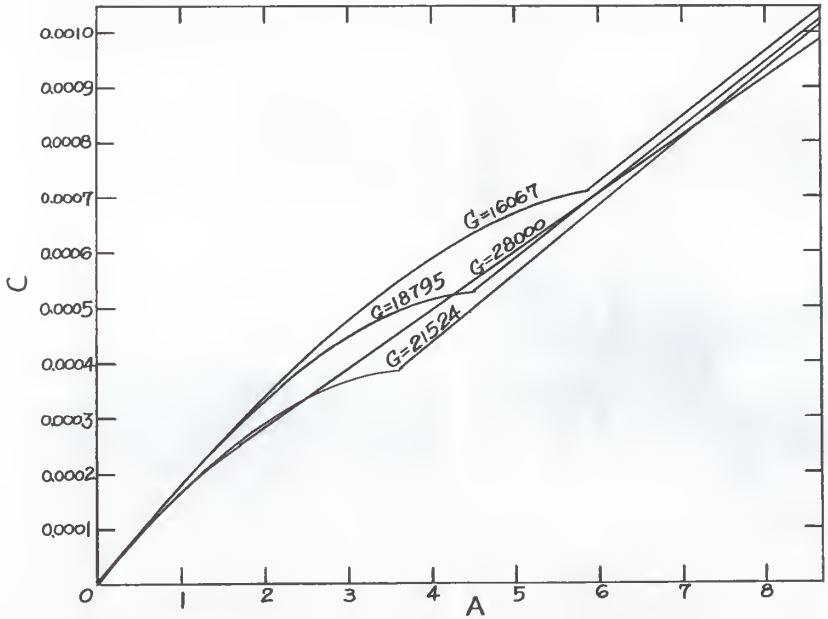
C
A
0.0010
0.0009
0.0008
0.0007
0.0006
0.0005
0.0004
0.0003
0.0002
0.0001
0
1
2
3
4
5
6
7
8
G=16067
G=18795
G=28000
G=21524

EXPLANATION OF PLATE XXVIII

Concentration gradient in semi-fluidized bed of benzoic acid-water system

Particle size: 20-24 mesh

Ordinate: C, Concentration, lb./lb.

Abscissa: A, Total particle surface, sq. ft.

PLATE XXVIII

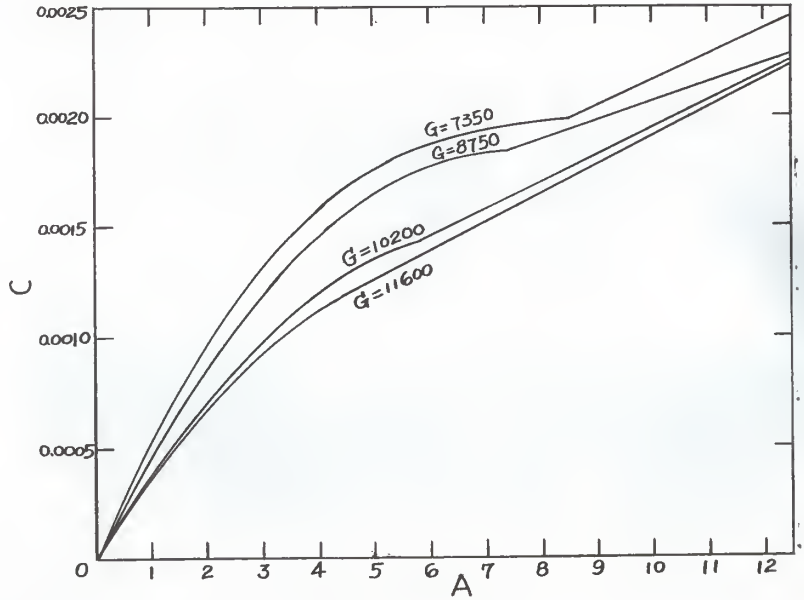

Table 2. Calculation of first series of semi-fluidized data.

Run No.	T Temperature °C	W Weight of Particle Bed lb.	h_o Height of Initial Bed ft.	h Overall Depth of Bed ft.	hf Height of Fluidized Bed Section ft.
A-1	22.3	0.4916	0.5888	0.8091	0.4008
2	20.0	0.4916	0.5888	0.8091	0.3508
3	20.0	0.4916	0.5888	0.8091	0.3258
4	20.0	0.4916	0.5888	0.8091	0.3758
5	21.2	0.4679	0.5603	0.8091	0.4425
6	21.5	0.4916	0.5888	1.2300	1.0925
7	21.5	0.4916	0.5888	1.2300	0.9925
8	20.1	0.2645	0.3168	None	0.9508
9	19.0	0.2645	0.3168	0.8258	0.7091
10	17.0	0.2645	0.3168	0.8258	0.7841
11	16.8	0.2645	0.3168	0.5008	0.2341
12	17.0	0.2645	0.3168	0.5008	0.2550
13	19.4	0.2645	0.3168	0.5008	0.2758
14	19.8	0.2645	0.3168	0.5008	0.3050
15	22.1	0.2645	0.3168	0.6675	0.5383
16	24.0	0.2645	0.3168	0.4350	0.1508
17	24.0	0.2645	0.3168	0.4350	0.1425
18	24.0	0.2645	0.3168	0.4350	0.1250
19	20.5	0.2645	0.3168	0.5008	0.3633
20	20.5	0.2645	0.3168	0.5008	0.2008
21	24.0	0.2645	0.3168	0.6617	0.4633
22	24.0	0.2645	0.3168	0.6617	0.3966
23	20.0	0.2645	0.3168	0.8258	0.6925
24	20.0	0.2645	0.3168	0.8258	0.5842
25	20.0	0.4864	0.5825	0.8091	0.3591
B-1	21.00	0.2533	0.2999	0.5008	0.3342
2	21.20	0.2533	0.2999	0.5008	0.2592
3	22.10	0.2533	0.2999	0.6633	0.5842
4	22.40	0.2533	0.2999	0.6633	0.5342
5	23.00	0.2533	0.2999	0.6633	0.5008
6	18.00	0.2646	0.3131	0.4783	1.4425
7	23.00	0.2646	0.3131	0.6258	0.4550
8	23.00	0.2646	0.3131	0.6258	0.4258
9	23.00	0.2646	0.3131	0.6258	0.4008
10	21.30	0.2646	0.3131	0.6258	0.3591
11	21.90	0.2646	0.3131	0.6633	0.4091
12	21.90	0.2646	0.3131	0.5225	0.2341
13	20.50	0.2646	0.3131	0.5225	0.2967
14	21.00	0.2493	0.2952	0.5008	0.3375
15	21.20	0.2487	0.2945	0.5008	0.2592
16	21.20	0.2441	0.2890	0.5008	0.2675

C-1	22.60	0.2645	0.3093	0.4675	0.2550
2	22.60	0.2645	0.3093	0.4675	0.2300
3	22.60	0.2645	0.3093	0.4675	0.2175
4	22.60	0.2645	0.3093	0.4675	0.1675
5	19.80	0.2645	0.3093	0.6342	0.5342
6	19.80	0.2645	0.3093	0.6342	0.5092
7	19.80	0.2645	0.3093	0.6342	0.4675
8	19.80	0.2645	0.3093	0.6342	0.4342
9	22.60	0.2585	0.3022	0.4675	0.2633
10	22.60	0.2572	0.3007	0.4675	0.2383
11	22.60	0.2566	0.3000	0.4675	0.2258
12	22.60	0.2552	0.2983	0.4675	0.1800
13	19.80	0.2576	0.3011	0.6342	0.5425
14	19.80	0.2570	0.3004	0.6342	0.5175
15	19.80	0.2559	0.2991	0.6342	0.4758
16	19.80	0.2556	0.2988	0.6342	0.4425

h_{pa} Height of Packed Bed Section ft.	X Weight Fraction in Packed Bed --	R Bed Expansion Ratio --	ϵ Overall Bed Porosity --	D_p Particle Diameter ft.	A Total Particle Surface Area ft^2
.0.4083	0.6935	1.3732	0.6548	0.00690	10.40
0.4583	0.7785	1.3732	0.6548	0.00690	10.42
0.4833	0.8208	1.3732	0.6548	0.00690	10.39
0.4333	0.7360	1.3732	0.6548	0.00690	10.40
0.3666	0.6542	1.4440	0.6717	0.00682	10.15
0.1375	0.2335	2.0902	0.7732	0.00690	10.41
0.2375	0.4034	2.0902	0.7732	0.00690	10.38
0	0			0.00690	5.60
0.1167	0.3683	2.6078	0.8182	0.00689	5.59
0.0417	0.1316	2.6078	0.8182	0.00690	5.60
0.2667	0.8420	1.5815	0.7002	0.00691	5.63
0.2458	0.7762	1.5815	0.7002	0.00689	5.57
0.2250	0.7104	1.5815	0.7002	0.00689	5.58
0.1958	0.6182	1.5815	0.7002	0.00689	5.58
0.1292	0.4080	2.1078	0.7751	0.00689	5.59
0.2842	0.8972	1.3732	0.6548	0.00688	5.57
0.2925	0.9233	1.3732	0.6548	0.00689	5.52
0.3100	0.9785	1.3732	0.6548	0.00685	5.53
0.1375	0.4341	1.5809	0.7002	0.00690	5.60
0.3000	0.9471	1.5809	0.7002	0.00688	5.58
0.1984	0.6265	2.0888	0.7731	0.00688	5.56
0.2651	0.8371	2.0888	0.7731	0.00686	5.53
0.1333	0.4207	2.6078	0.8182	0.00690	5.59
0.2416	0.7625	2.6078	0.8182	0.00688	5.57
0.4500	0.7725	1.3890	0.6587	0.00688	10.42
0.1666	0.5555	1.6700	0.7129	0.004531	7.62
0.2416	0.8054	1.6700	0.7129	0.004532	7.60
0.0791	0.2637	2.2118	0.7832	0.004523	7.57
0.1291	0.4303	2.2118	0.7832	0.004529	7.59
0.1625	0.5416	2.2118	0.7832	0.004520	7.56
0.0358	0.1148	4.7218	0.8985	0.004532	7.59
0.1708	0.5454	1.9987	1.7601	0.004523	7.92
0.2000	0.6383	1.9987	0.7601	0.004516	7.90
0.2250	0.7180	1.9987	0.7601	0.004513	7.89
0.2667	0.8510	1.9987	0.7601	0.004509	7.87
0.2542	0.8114	2.1185	0.7737	0.004509	7.87
0.2884	0.9206	1.6688	0.7127	0.004505	7.86
0.2258	0.7207	1.6688	0.7127	0.004523	7.92
0.1633	0.5532	1.6965	0.7174	0.00451	7.53
0.2416	0.8203	1.7005	0.7180	0.004450	7.50
0.2333	0.8071	1.7328	0.7233	0.00448	7.41

0.2125	0.6873	1.5114	0.6787	0.002610	12.50
0.2375	0.7682	1.5114	0.6787	0.002606	12.46
0.2500	0.8083	1.5114	0.6787	0.002603	12.44
0.3000	0.9701	1.5114	0.6787	0.002598	12.39
0.1000	0.3232	2.0504	0.7632	0.002609	12.47
0.1250	0.4041	2.0504	0.7632	0.002604	12.46
0.1667	0.5391	2.0504	0.7632	0.002600	12.42
0.2000	0.6469	2.0504	0.7632	0.002599	12.40
0.2042	0.6758	1.5470	0.6861	0.002602	12.38
0.2292	0.7624	1.5547	0.6876	0.002591	12.30
0.2417	0.8059	1.5583	0.6884	0.002585	12.25
0.2875	0.9636	1.5672	0.6901	0.002572	12.17
0.0917	0.3044	2.1062	0.7694	0.002592	12.32
0.1167	0.3883	2.1111	0.7700	0.002592	12.27
0.1584	0.5295	2.1203	0.7710	0.002580	12.20
0.1917	0.6416	2.1224	0.7712	0.002578	12.18

G Superficial Mass Velocity lb/(hr)(ft^2)	G' Mass Velocity lb/hr	C_s Saturated Concentration lb/lb	C_2 Outlet Concentration lb/lb	$(k_L)_{l.m.}$ Mass Transfer Coefficient lb/(hr)(ft^2)(Δ C)	N_{Sc} Schmidt Number --
16067	350.52	0.003140	0.001640	24.90	1120
13338	290.98	0.002902	0.001618	22.77	1290
18795	410.03	0.002902	0.001483	28.32	1290
16067	350.52	0.002902	0.001587	26.62	1290
13338	290.98	0.003025	0.001136	17.58	1200
21524	496.57	0.003057	0.001158	21.48	1180
24150	529.04	0.003057	0.001189	24.89	1180
30400	663.21	0.002907	0.000446	19.71	1290
33000	719.93	0.002803	0.000496	25.10	1360
28000	610.85	0.002619	0.000434	19.88	1530
33000	719.93	0.002600	0.000628	34.72	1540
28000	610.85	0.002619	0.000644	30.92	1530
24150	496.57	0.002842	0.000700	23.77	1335
21504	528.04	0.002878	0.000758	28.87	1300
28000	610.85	0.003121	0.000676	26.64	1140
24150	469.57	0.003336	0.000952	27.29	1020
31000	676.30	0.003336	0.000949	41.03	1020
39600	863.92	0.003336	0.000882	47.98	1020
18795	410.03	0.002907	0.000675	19.31	1250
39600	863.91	0.002907	0.000550	32.46	1250
31000	676.30	0.003336	0.000799	33.31	1020
39600	863.91	0.003336	0.000835	44.71	1020
31000	676.30	0.002902	0.000488	22.29	1290
39600	863.91	0.002902	0.000570	33.84	1290
13338	290.98	0.002902	0.001551	21.51	1290
10610	231.47	0.003005	0.001563	22.30	1220
13338	290.98	0.003024	0.001437	28.42	1200
16067	350.52	0.003121	0.001137	20.89	1140
18795	410.03	0.003154	0.001127	24.04	1120
21524	469.57	0.003223	0.001197	28.81	1080
30400	663.20	0.002709	0.000635	23.59	1140
18795	410.03	0.003223	0.001399	29.63	1080
21524	469.57	0.003223	0.001380	33.25	1080
24150	529.04	0.003223	0.001380	37.55	1080
28000	610.85	0.003036	0.001286	42.69	1200
28000	610.85	0.003100	0.001260	40.35	1160
28000	610.85	0.003100	0.001395	46.56	1160
21524	469.57	0.002953	0.001209	31.17	1250
10610	231.47	0.003005	0.001508	21.37	1220
13338	290.98	0.003024	0.001437	28.79	1200
13338	290.98	0.003024	0.001408	24.93	1200

4500	98.17	0.003177	0.003051	25.38	1110
6450	140.71	0.003177	0.002968	29.98	1110
7700	167.98	0.003177	0.002812	27.58	1110
10000	218.16	0.003177	0.002719	31.38	1110
7350	160.35	0.002882	0.002387	20.24	1300
8750	190.89	0.002882	0.002267	20.00	1300
10200	222.52	0.002882	0.002402	28.84	1300
11600	253.06	0.002882	0.002226	25.08	1300
4500	98.17	0.003177	0.002968	21.05	1110
6450	140.71	0.003177	0.002864	24.48	1110
7700	167.98	0.003177	0.002802	27.58	1110
10000	218.16	0.003177	0.002657	29.26	1110
7350	160.35	0.002882	0.002350	19.35	1300
8750	190.89	0.002882	0.002257	19.97	1300
10200	222.52	0.002882	0.002361	27.57	1300
11600	253.06	0.002882	0.002200	24.30	1300

N_{Sh} Sherwood Number	N'_{Re} Modified Rsynolds Number	$N'_{Re}/(1-\epsilon)$ Dimensionless Group	J_d Mass Transfer Factor	$(N_{Sh}\epsilon^{-2})/N_{Sc}^{1/3}$ Dimensionless Group	J'_d Modified Mass Transfer Factor
64.48	48.33	140.0	0.1670	3.87	0.1245
63.84	37.89	109.7	0.2023	3.66	0.1500
79.42	53.36	154.5	0.1785	4.60	0.1333
74.64	45.93	133.0	0.1964	4.31	0.1454
46.46	38.14	115.7	0.1525	2.73	0.1084
57.34	63.48	280.0	0.1115	3.66	0.0753
66.41	71.52	315.4	0.1146	4.67	0.0852
54.36	86.33	546.7	0.0768	4.08	0.0574
72.59	91.30	502.4	0.0933	5.18	0.0698
61.80	85.47	470.3	0.0943	4.22	0.0607
108.88	86.57	288.4	0.1403	6.43	0.1070
96.00	85.35	284.8	0.1466	5.66	0.0955
67.85	67.41	224.8	0.1193	4.32	0.0887
81.36	60.67	202.3	0.1597	5.22	0.1295
69.55	83.21	370.2	0.1003	5.97	0.0778
66.55	75.11	217.6	0.1145	4.13	0.0860
100.20	96.56	279.7	0.1342	6.32	0.1030
116.50	122.63	355.2	0.1228	7.38	0.0935
53.27	53.97	180.0	0.1192	3.28	0.0884
89.29	113.38	378.1	0.0965	5.62	0.0721
81.24	96.42	424.9	0.1089	6.04	0.0818
108.72	122.81	541.2	0.1144	8.16	0.0864
62.51	87.81	483.0	0.0852	4.52	0.0686
94.63	111.85	615.2	0.1012	6.98	0.0765
60.14	37.73	110.50	0.1911	3.64	0.1416
39.74	20.25	70.53	0.2400	2.46	0.1745
50.29	25.58	89.09	0.2405	3.18	0.1778
35.88	31.42	144.92	0.1423	2.49	0.1030
40.77	37.06	170.94	0.1380	2.88	0.1002
47.75	42.96	198.15	0.1409	3.45	0.1038
46.47	53.92	531.23	0.0989	3.52	0.0730
49.24	37.53	156.44	0.1660	3.46	0.1230
55.05	42.92	178.90	0.1620	4.08	0.1202
62.14	48.13	200.62	0.1637	4.41	0.1219
74.89	53.56	223.25	0.1721	5.17	0.1280
69.43	54.32	240.03	0.1590	4.93	0.1357
80.04	54.28	188.93	0.1835	5.24	0.1370
56.36	40.51	141.00	0.1680	3.54	0.1246
37.94	20.16	71.33	0.2300	2.55	0.1669
50.60	25.40	90.07	0.2437	3.23	0.1800
43.60	25.28	91.36	0.2110	2.78	0.1547

24.63	5.138	15.99	0.6045	1.61	0.4255
29.05	7.352	22.88	0.4982	1.71	0.3554
26.69	8.768	27.09	0.3839	1.56	0.2721
30.31	11.365	35.37	0.3363	1.79	0.2407
21.60	7.845	33.13	0.3279	1.33	0.2290
21.30	9.322	39.37	0.2790	1.31	0.1897
30.67	10.850	45.82	0.3367	1.96	0.2421
26.66	12.334	52.09	0.2574	1.68	0.1832
20.36	5.122	16.32	0.5014	1.16	0.3463
24.96	7.310	23.40	0.4068	1.46	0.3045
26.51	8.707	27.94	0.3839	1.57	0.2720
27.98	11.251	36.31	0.3136	1.67	0.2230
20.52	7.794	33.80	0.3134	1.26	0.2178
21.17	9.279	40.34	0.2873	1.31	0.1894
29.09	10.766	47.01	0.3219	1.87	0.2306
25.62	12.235	53.47	0.2494	1.63	0.1769

Table 3. Calculation of second series of semi-fluidized bed data.

Run No	W Weight of bed lb.	h_o Height of bed ft.	h Overall depth of bed ft.	h_f Height of fluidized bed section ft.
D-1	0.3307	0.3613	0.5717	0.3484
D-2	0.3307	0.3613	0.5717	0.3151
D-3	0.3307	0.3613	0.5717	0.2913
D-4	0.3307	0.3613	0.5717	0.2676
E-1	0.2899	0.3131	0.6667	0.5650
E-2	0.2899	0.3131	0.6667	0.5158
E-3	0.2899	0.3131	0.6667	0.4833
E-4	0.2899	0.3131	0.6667	0.4125
F-1	0.2645	0.2851	0.5833	0.4921
F-2	0.2645	0.2851	0.5833	0.4693
F-3	0.2645	0.2851	0.5833	0.4313
F-4	0.2645	0.2851	0.5833	0.4009

pa ght of ked bed tion ft.	X Weight fraction in packed bed section --	D_p Particle diameter ft.	A Total particle surface sq.ft.	ϵ Porosity --	S Cross-section Area of Column sq.ft.
.2233	0.6182	0.006890	6.97	0.7004	0.023916
.2566	0.7104	0.006890	6.97	0.7004	"
.2804	0.7762	0.006890	6.97	0.7004	"
.3041	0.8420	0.006890	6.97	0.7004	"
.1017	0.3240	0.004530	8.68	0.7740	"
.1509	0.4800	0.004523	8.65	0.7740	"
.1834	0.5830	0.004520	8.64	0.7740	"
.2542	0.8110	0.004510	8.60	0.7740	"
.0912	0.3232	0.002609	12.47	0.7617	"
.1140	0.4041	0.002604	12.46	0.7617	"
.1520	0.5391	0.002600	12.40	0.7617	"
.1824	0.6469	0.002599	12.40	0.7617	"

Height of sampling outlet ft.			C Concentration, lb/lb. at			C_1 Conc. at interface lb/lb	C_2 Conc. at outlet lb/lb
a	b	c	a	b	c		
0.2033	0.3700	0.5717	0.000215	0.000359	0.000943	0.00030	0.000943
0.2033	0.3700	0.5717	0.000161	0.000287	0.000862	0.00021	0.000862
0.2033	0.3700	0.5717	0.000107	0.000251	0.000799	0.00012	0.000799
0.2033	0.3700	0.5717	0.000099	0.000242	0.000745	0.00007	0.000745
0.3700	0.5367	0.6667	0.000585	0.000690	0.001044	0.00071	0.001044
0.3700	0.5367	0.6667	0.000456	0.000591	0.001027	0.00053	0.001027
0.3700	0.5367	0.6667	0.000363	0.000580	0.001017	0.00039	0.001017
0.3700	0.5367	0.6667	0.000244	0.000623	0.000992	0.00025	0.000992
0.2033	0.3700	0.5833	0.001428	0.001921	0.002460	0.00198	0.002460
0.2033	0.3700	0.5833	0.001383	0.001886	0.002280	0.00184	0.002280
0.2033	0.3700	0.5833	0.001033	0.001364	0.002263	0.00142	0.002263
0.2033	0.3700	0.5833	0.000970	0.001176	0.002245	0.00118	0.002245

Saturated concentration lb/lb	$(\Delta C)_{l.m.}$			$(\Delta C)_{t.m.}$		
	Packed bed section	Fluidized bed section	Overall	Packed bed section	Fluidized bed section	Overall
0.002902	0.002271	0.002752	0.002405	0.002380	0.002752	0.002460
0.002902	0.002385	0.002763	0.002480	0.002397	0.002792	0.002511
0.002902	0.002470	0.002842	0.002505	0.002474	0.002842	0.002556
0.002902	0.002466	0.002862	0.002515	0.002499	0.002862	0.002651
0.002953	0.002640	0.002590	0.002367	0.002076	0.002507	0.002556
0.002953	0.002240	0.002780	0.002414	0.002272	0.002703	0.002567
0.002953	0.002240	0.002760	0.002428	0.002224	0.002743	0.002722
0.002953	0.002270	0.002790	0.002439	0.002260	0.002731	0.002725
0.003223	0.000883	0.002077	0.001709	0.001003	0.001943	0.001639
0.003223	0.001160	0.002175	0.001846	0.001171	0.002010	0.001671
0.003223	0.001329	0.002435	0.001854	0.001371	0.002347	0.001821
0.003223	0.001445	0.002582	0.001880	0.001510	0.002453	0.001843

G Mass velocity lb/(hr)(sq.ft.)	G' Mass velocity lb/hr	(k_L)l.m. Packed bed section	(k_L)l.m. Fluidized bed section	(k_L)l.m. Overall	(k_L)t.m. Packed bed section	(k_L)t.m. Fluidized bed section	(k_L)t.m. Overall
21524	514.77	30.83	21.08	28.97	28.68	21.08	28.32
24150	577.57	30.87	21.75	28.81	30.83	21.52	28.45
28000	669.65	33.83	18.14	30.66	33.70	18.14	30.04
33000	789.22	36.32	17.53	33.56	35.85	17.53	31.83
16067	384.26	30.10	13.28	19.57	20.70	13.71	18.08
18795	449.59	22.25	17.85	22.10	21.90	18.40	20.79
21524	514.77	26.30	22.70	24.93	26.50	22.40	22.24
28000	669.65	28.20	33.00	31.67	28.30	24.30	25.35
7350	175.78	21.31	19.85	20.29	21.88	20.88	21.15
8750	209.26	18.15	23.82	20.74	23.77	20.71	22.91
10200	243.94	23.49	24.74	24.98	24.74	22.77	24.41
11600	277.42	25.33	28.82	26.24	28.52	24.25	26.77

N'_{Re} Reynolds number	$N'_{Re}/(1-\epsilon)$ Dimensionless group	N_{Sh} Sherwood number		J_d Mass-transfer coefficient	
		Log. mean driving force	Integrated mean driving force	Log. mean driving force	Integrated mean driving force
60.88	203.30	81.00	79.3	0.1588	0.1552
68.31	228.00	80.6	79.6	0.1407	0.1390
79.20	264.35	85.8	84.1	0.1292	0.1265
93.34	311.54	94.0	89.0	0.1199	0.1137
31.40	139.00	35.4	32.7	0.1413	0.1305
35.50	159.00	40.0	37.6	0.1363	0.1283
40.50	179.10	45.1	40.3	0.1343	0.1198
52.60	233.00	57.3	51.3	0.1312	0.1174
8.47	35.54	19.4	20.2	0.2907	0.3030
10.06	42.21	22.9	21.9	0.2495	0.2756
11.71	49.14	19.8	23.3	0.2475	0.2519
13.31	55.85	25.1	25.6	0.2381	0.2430

N_{Sc} Schmidt number	$(N_{Sh}\epsilon - 2)/N_{Sc}^{1/3}$ Dimensionless group		J'_d Modified mass-transfer coefficient	
	Log. mean driving force	Integrated mean driving force	Log. mean driving force	driving force
1290	5.03	4.91	0.1192	0.1167
1290	5.00	4.94	0.1057	0.1044
1290	5.34	5.23	0.0972	0.0953
1290	5.86	5.54	0.0906	0.0857
1250	2.36	3.16	0.0987	0.0908
1250	2.69	2.52	0.0994	0.0931
1250	3.05	2.71	0.0988	0.0878
1250	3.94	3.50	0.0976	0.0870
1080	1.25	1.30	0.2004	0.2097
1080	1.27	1.43	0.1726	0.1930
1080	1.51	1.54	0.1742	0.1775
1080	1.67	1.71	0.1693	0.1693

Table 4. Results of recalculation of Evan and Gerald's fluidized bed data (8).

Run No.	T : Temperature : °C	Weight of Particle Bed lb.	h_f : Height of Fluidized Bed ft.	D_p : Particle Diameter ft.	ϵ : Porosity --
1	24.00	0.1012	0.141	0.00660	0.56
2	24.05	0.1009	0.151	0.00664	0.59
3	23.41	0.1050	0.193	0.00678	0.67
4	24.70	0.1021	0.200	0.00668	0.69
5	24.70	0.1039	0.272	0.00670	0.77
6	23.40	0.1061	0.295	0.00678	0.78
7	23.40	0.0601	0.121	0.00434	0.70
8	22.70	0.0616	0.131	0.00438	0.71
9	23.05	0.0640	0.108	0.00442	0.69
10	23.56	0.0606	0.144	0.00434	0.75
11	23.33	0.0376	0.095	0.00392	0.76
12	23.35	0.0569	0.193	0.00426	0.82
13	23.42	0.0572	0.262	0.00426	0.87
14	23.65	0.0583	0.082	0.00249	0.56
15	23.75	0.0589	0.082	0.00248	0.56
16	23.81	0.0565	0.084	0.00245	0.59
17	23.70	0.0492	0.082	0.00209	0.63
18	22.07	0.0951	0.182	0.00249	0.68
19	23.61	0.0906	0.226	0.00246	0.75
20	23.29	0.0875	0.292	0.00242	0.82
21	24.73	0.0854	0.446	0.00238	0.88
22	24.20	0.0836	0.573	0.00242	0.91
23	24.07	0.0625	0.115	0.00179	0.67
24	23.40	0.0303	0.072	0.00182	0.74
25	23.41	0.0307	0.415	0.00180	0.91

G Superficial Mass Velocity lb/(hr)(ft^2)	C_s Saturated Concentration lb/lb	C_2 Outlet Concentration lb/lb	$(kL)_{l.m.}$ Mass Transfer Coefficient lb/(hr)(ft^2)(ΔC)	N_{Sc} Schmidt Number --	N_{Sh} Sherwood Number --
3300	0.00328	0.001120	12.6	1020	29.42
8650	0.00328	0.000594	15.9	1020	37.21
11420	0.00321	0.000462	15.9	1060	38.98
15200	0.00373	0.000405	15.7	385	36.20
21870	0.00373	0.000316	16.8	385	38.84
23750	0.00321	0.000274	18.9	1060	46.35
8320	0.00321	0.000552	16.2	1060	25.42
11150	0.00313	0.000432	17.6	1100	28.60
11420	0.00317	0.000467	18.9	1080	30.63
13590	0.00323	0.000380	18.6	1050	29.02
13600	0.00320	0.000290	21.8	1060	30.98
19600	0.00320	0.000268	20.2	1060	31.19
23000	0.00321	0.000269	23.4	1060	36.01
1381	0.00324	0.002200	11.4	1040	10.17
1386	0.00325	0.002068	10.0	1040	8.86
3020	0.00326	0.001460	13.3	1030	11.61
3890	0.00324	0.001290	15.6	1040	11.66
5840	0.00315	0.001531	17.2	1100	15.77
8380	0.00324	0.001303	20.2	1040	17.85
11510	0.00320	0.001040	20.6	1070	18.08
14950	0.00337	0.000930	20.2	390	16.58
17490	0.00330	0.000796	23.5	1015	19.99
3400	0.00318	0.001739	14.2	1085	9.30
6620	0.00321	0.000704	17.7	1060	11.65
8320	0.00321	0.000589	17.7	1060	11.52

N'_{Re} Modified Reynolds Number --	$\frac{N'_{Re}}{1-\epsilon}$ Dimensionless Group --	J_d Mass Transfer Factor --	$\frac{N_{Sh}\epsilon^{-2}}{N_{Sc}^{1/3}}$ Dimensionless Group --	J'_d Modified Mass Transfer Factor --
9.80	22.27	0.390	1.43	0.276
25.80	62.92	0.188	1.98	0.135
34.60	104.84	0.146	2.36	0.104
46.50	150.00	0.102	2.30	0.074
67.20	292.17	0.076	2.80	0.055
71.6	325.45	0.084	3.34	0.061
16.0	53.33	0.204	1.54	0.143
21.3	73.44	0.170	1.77	0.120
22.2	71.61	0.175	1.86	0.125
26.2	104.80	0.142	1.94	0.105
23.6	98.33	0.168	2.10	0.120
37.0	205.50	0.108	2.30	0.077
43.4	333.84	0.106	2.87	0.077
1.58	3.59	0.855	0.36	0.505
1.53	3.47	0.745	0.29	0.437
3.32	8.09	0.453	0.48	0.286
3.62	9.78	0.414	0.53	0.262
6.40	20.00	0.314	0.84	0.208
9.20	36.80	0.250	1.12	0.169
12.3	68.33	0.188	1.25	0.127
16.3	135.8	0.134	1.26	0.090
19.1	212.2	0.136	1.61	0.093
2.69	8.15	0.442	0.41	0.264
5.34	20.54	0.280	0.65	0.176
6.66	74.00	0.222	0.83	0.139

Table 5. Results of recalculation of Evan and Gerald's packed bed data (8).

Run No.	T Temperature °C	W Weight of Particle Bed lb.	h_{pa} Height of Fluidized Bed ft.	D_p Particle Diameter ft.	ϵ Porosity --
1	23.49	0.1039	0.138	0.00676	0.54
2	23.52	0.1038	0.130	0.00667	0.51
3	23.60	0.1060	0.132	0.00673	0.51
4	23.40	0.1033	0.131	0.00672	0.52
5	23.60	0.1010	0.122	0.00664	0.51
6	23.70	0.0619	0.079	0.00433	0.53
7	23.30	0.0642	0.081	0.00440	0.51
8	23.10	0.0629	0.083	0.00435	0.54
9	23.91	0.0586	0.085	0.00431	0.58
10	23.60	0.0512	0.082	0.00418	0.62
11	23.40	0.0654	0.079	0.00447	0.49
12	23.50	0.0610	0.076	0.00434	0.50
13	23.89	0.1058	0.129	0.00256	0.50
14	23.40	0.0596	0.071	0.00249	0.49
15	23.40	0.0590	0.076	0.00248	0.52
16	23.61	0.0479	0.062	0.00230	0.50
17	23.10	0.0621	0.079	0.00183	0.52
18	23.71	0.0853	0.098	0.00182	0.47

G Superficial Mass Velocity lb/(hr)(ft^2)	C_s Saturated Concentration lb/lb	C_2 Outlet Concentration lb/lb	$(k_L)_{l.m.}$ Mass Transfer Coefficient lb/(hr)(ft^2)(Δ C)	N_{Sc} Schmidt Number --	N_{Sh} Sherwood Number --
2345	0.00322	0.001475	12.8	1050	31.15
2870	0.00322	0.001280	13.1	1050	31.41
8660	0.00323	0.000805	21.6	1045	52.21
15220	0.00321	0.000588	27.2	1060	66.11
19410	0.00323	0.000562	35.2	1045	83.97
1386	0.00324	0.001820	12.5	1040	19.35
1843	0.00320	0.001665	15.8	1065	22.00
4205	0.00318	0.001119	19.0	1080	30.20
4625	0.00327	0.000950	18.0	1030	28.53
17780	0.00324	0.000580	43.4	1045	65.16
18620	0.00321	0.000628	41.1	1060	66.44
22400	0.00322	0.000585	48.0	1050	75.00
1669	0.00315	0.002945	18.1	1030	17.03
14000	0.00321	0.001325	52.5	1060	47.28
16680	0.00321	0.001210	55.5	1060	49.78
17780	0.00322	0.001031	54.6	1045	45.11
1148	0.00318	0.002990	17.4	1080	11.63
3060	0.00324	0.002830	24.3	1040	15.81

N'_{Re} Modified Reynolds Number	$\frac{N'_{Re}}{1-\epsilon}$ Dimensionless Group	J_d Mass Transfer Factor	$\frac{N_{Sh}\epsilon^{-2}}{N_{Sc}^{1/3}}$ Dimensionless Group	J'_d Modified Mass Transfer Factor
7.09	15.41	0.545	1.45	0.401
8.53	17.40	0.476	1.37	0.438
26.0	53.06	0.259	2.41	0.189
45.5	94.79	0.187	3.17	0.138
57.5	117.34	0.190	3.99	0.139
2.68	5.70	0.942	0.81	0.638
3.58	7.30	0.785	0.90	0.545
8.09	17.58	0.478	1.39	0.339
8.74	20.80	0.415	1.41	0.297
33.0	86.84	0.260	3.76	0.187
37.0	72.55	0.230	2.99	0.171
43.2	86.40	0.223	3.48	9.165
1.87	3.74	1.16	0.63	0.772
15.5	30.39	0.392	2.07	0.288
18.5	38.54	0.348	2.33	0.252
18.1	36.20	0.318	2.02	0.234
0.92	1.91	1.60	0.39	1.020
2.48	4.67	0.820	0.53	0.505

MASS TRANSFER IN SEMI-FLUIDIZED BEDS

by

Yung Chia Yang

B. S., National Taiwan University, China, 1955

AN ABSTRACT OF A THESIS

submitted in partial fulfillment of the

requirements for the degree

MASTER OF SCIENCE

Department of Chemical Engineering

KANSAS STATE UNIVERSITY
OF AGRICULTURE AND APPLIED SCIENCE

1959

Semi-fluidization is a new fluid-solid contact process in which two distinct beds of the solid particles are formed simultaneouely within a single vessel. This can be accomplished by partial restriction or prevention of the bed expansion of the fluidized bed. Two types of the solid particles beds formed in the semi-fluidized operation are a packed bed and a fluidized bed. Therefore, the semi-fluidized bed should possess the characteristics of both the packed bed and the fluidized bed. In this investigation, the mass-transfer aspect of semi-fluidization was investigated by use of the benzoic acid-water system.

Several dimensionless correlatione were obtained based on the overall mean driving force. It was found that the correlations obtained are very similar to those for the ordinary packed and fluidized beds.

As a matter of fact, these correlations can be used in calculation of the overall mass-transfer coefficients in the semi-fluidized bed for purpose of approximation. However, the porosity of the semi-fluidized bed is an independent variable of the operation unlike that of ordinary fluidized bed. In other words, the rate of mass-transfer can be controlled by means of the bed expansion only.

Some additional experiments were conducted in order to study the effect of axial mixing on the overall mass transfer correlation and also the effect of sudden change in the concentration gradient. It was found that such effecte were small.

It was also shown that the overall mean k_L is expressed as a linear combination of effective kL of each bed.